Título artículo / Títol article:	High precision Symplectic Integrators for the Solar System
Autores / Autors	Farrés Basiana, Ariadna ; Laskar, Jacques ; Blanes, Sergio ; Casas Pérez, Fernando ; Makazaga, Joseba ; Murua, Ander
Revista:	Celestial Mechanics and Dynamical Astronomy, 2013, vol. 116, no. 2
Versión / Versió:	Preprint del autor
Cita bibliográfica / Cita bibliogràfica (ISO 690):	FARRÉS, Ariadna, et al. High precision symplectic integrators for the Solar System. Celestial Mechanics and Dynamical Astronomy, 2013, vol. 116, no 2, p. 141-174
url Repositori UJI:	http://hdl.handle.net/10234/83769

Celestial Mechanics and Dynamical Astronomy manuscript No.
(will be inserted by the editor)

High precision Symplectic Integrators for the Solar System

Ariadna Farrés · Jacques Laskar · Sergio Blanes · Fernando Casas · Joseba Makazaga · Ander Murua

Received: date / Accepted: date

Abstract Using a Newtonian model of the Solar System with all 8 planets, we perform extensive tests on various symplectic integrators of high orders, searching for the best splitting scheme for long term studies in the Solar System. These comparisons are made in Jacobi and Heliocentric coordinates and the implementation of the algorithms is fully detailed for practical use. We conclude that high order integrators should be privileged, with a preference for the new $(10, 6, 4)$ method of (Blanes et al, 2012).

Keywords symplectic integrators · Hamiltonian systems · planetary motion

1 Introduction

Due to their simplicity and stability properties, symplectic integrators have been widely used for long-term integrations of the Solar System, starting with the work of Wisdom and Holman (1991). In many studies on the formation and evolution of the Solar System, where large numbers of particles are considered, the speed of the integrator is a major constraint and low order schemes have been often privileged as in the original scheme of (Wisdom and Holman, 1991) or (Kinoshita et al, 1991) (for a review see (Morbidelli, 2002)).

Ariadna Farrés · Jacques Laskar
Astronomie et Systèmes Dynamiques, IMCCE-CNRS UMR8028, Observatoire de Paris, UPMC,, 77 Av. Denfert-Rochereau, 75014-Paris, France E-mail: afarres@imcce.fr, laskar@imcce.fr

Sergio Blanes
Instituto de Matemática Multidisciplinar, Universitat Politécnica de València, 46022-Valencia, Spain E-mail: serblaza@imm.upv.es

Fernando Casas
Institut de Matemàtiques i Aplicacions de Castelló and Departament de Matemàtiques, Universitat Jaume I, E-12071 Castellón, Spain E-mail: Fernando.Casas@uji.es

Joseba Makazaga · Ander Murua
Konputazio Zientziak eta A.A. saila, Informatika Fakultatea, EHU/UPV, Donostia/San Sebastián, Spain E-mail: Joseba.Makazaga@ehu.es, Ander.Murua@ehu.es

On the opposite, in the present work we are focusing on high precision symplectic integrators that are designed for the computation of long term ephemerides of the Solar System, when one searches to reduce the numerical error of the algorithm to the level of the roundoff error of the machine. These integrators will also be useful for the detailed dynamical studies of the extra solar planetary system with strong planetary interactions.

The first long term direct numerical integration of a realistic model of the Solar System, including all planets and the effects of general relativity and the Moon was made twenty years ago over 3 Myr (Quinn et al, 1991) using a high order symmetric multistep method. This solution could be compared with success with the previous averaged solutions of (Laskar, 1989, 1990a) and confirmed the existence of secular resonances in the Solar System (Laskar et al, 1992). Soon after, using a symplectic integrator with mixed variables (Wisdom and Holman, 1991), Sussman and Wisdom (1992) could extend these computation to 100 Myr, confirming the chaotic behaviour of the Solar System discovered with the secular equations by Laskar (1989, 1990a).

As the Solar System is chaotic, the error in numerical integrations is multiplied by 10 every 10 Myr (Laskar, 1989). Due to the limited accuracy of the models and initial conditions, it is thus hopeless to obtain a precise solution for the evolution of the Solar System over more than 100 Myr. The situation is even worse when the full Solar System is considered, as close encounters among the minor planets induce strong chaotic effects that will limit all possibilities of computing a precise solution for the planets to about 60 Myr (Laskar et al, 2011a,b).

Despite this limitation, there is a strong need for precise ephemerides of the planets from the paleoclimate community. Indeed, the variations of the Earth orbital elements induce some changes in the Earth climate that are reflected in the sedimentary records over million of years. This mechanism, known as Milankovitch theory (Milankovitch, 1941) allows now to use the astronomical solution for the calibration of the geological time scales through the correlation of the variation of orbital and rotational elements of the Earth to geological records. This method has been successfully used for the Neogene period (Lourens et al, 2004) over 23 Myr, and a large effort is pursued at present to extend this study over the full Cenozoic era, up to about 65 Myr. This quest led to search for high order symplectic schemes that are adapted to these long time computations, where high accuracy is requested Laskar and Robutel (2001); Laskar et al (2004, 2011a), but it should be noted that in the latest work, the integration of the Solar System model over 250 Myr[1], including five main asteroids took more than 18 months of CPU time. Some improvements of the algorithms were thus needed, and the present paper is the outcome of the studies that we have understaken in order to search for the best integrators for the next generations of numerical solutions. At the same time, we have compared various sets of coordinates (Heliocentrics and Jacobi), as the performances of these integrators depend on the choice of splitting of the Hamiltonian, and thus of the set of coordinates that correspond to these various splittings. As the integrators that are presented here are of high order, they

[1] Although it has been demonstrated that a precise solution of the motion of the Earth cannot be computed over more than 60 Myr (Laskar et al, 2011b), the solutions are systematically computed over 250 Myr as some features of the solutions can be trusted over longer times Laskar et al (2004, 2011a).

can also be used for refined analysis of the newly discovered extra solar planetary systems, especially when the planetary interactions in the system are strong.

For the planetary case, when using an appropriate set of coordinates, the equations of motion are written as an integrable part H_A, that corresponds to the Keplerian motion of each planet, and a small perturbation H_B, given by the interaction of the planets between each other. Hence, the system falls into the category of Hamiltonian system of the kind $H = H_A + \varepsilon H_B$.

Several splitting integrating schemes that take advantage of this fact to derive efficient integrators exist in the literature. McLachlan (1995) was the first to present such schemes and was followed independently by Chambers and Murison (2000) and Laskar and Robutel (2001). Most recently works by Blanes et al (2012) derived higher order schemes that present very interesting behaviour.

In this paper we describe these different splitting symplectic schemes and compare them for the case of the Solar System dynamics. We want to see which are the most efficient and accurate schemes. We will consider the gravitational N-body model and test the different integrating schemes against different planetary configurations, to be more specific: the 4 inner planets, the 4 outer planets and the 8 planets in the Solar System (Section 4).

The Hamiltonian of the gravitational N-body problem $H = T(p) + U(q)$ can be rewrite as $H = H_A + \varepsilon H_B$, using to different set of canonical coordinates: Jacobi and Heliocentric coordinates (Section 3). The main difference between both set of equations is that in Jacobi coordinates the small perturbation H_B depends only in positions while in Heliocentric coordinates these one depends on both position and velocity. This is why in the literature Jacobi coordinates have been more widely used. In Section 5 we describe different symplectic schemes for Jacobi coordinates, and in Section 6 other symplectic schemes that are suitable for Heliocentric coordinates. In both Sections we describe and compare the different splitting schemes. Finally in Section 7 we compare the results for the two different set of coordinates.

2 Splitting Symplectic Integrators (General Overview)

Let $H(q,p)$ be a Hamiltonian system where (q,p) are a set of canonical coordinates (i.e. q are the positions and p the momenta). It is well known that in many mechanical problems the Hamiltonian is of the form

$$H(q,p) = T(p) + U(q),$$

which is separable with respect to the local canonical coordinates. Using the Lie formalism we can write the equations of motion as:

$$\frac{dz}{dt} = \{H, z\} = L_H z, \tag{1}$$

where by definition $L_\chi f := \{\chi, f\}$ is the differential operator L_χ, $z = (q,p)$ and $\{\cdot,\cdot\}$ denotes the Poisson bracket[2].

The formal solution of Eq. 1 at time $t = \tau_0 + \tau$ that starts at time $t = \tau_0$ is given by

$$z(\tau_0 + \tau) = \exp(\tau L_H) z(\tau_0) = \exp(\tau(L_T + L_U)) z(\tau_0). \tag{2}$$

[2] $\{F,G\} = \sum_{i=1}^{n} \frac{\partial F}{\partial p_i}\frac{\partial G}{\partial q_i} - \frac{\partial F}{\partial q_i}\frac{\partial G}{\partial p_i}$

In general the operators L_T and L_U do not commute, $\exp(\tau(L_T + L_U)) \neq \exp(\tau L_T)\exp(\tau L_U)$, but we can find coefficients a_i, b_i such that for a given r,

$$\exp(\tau(L_T + L_U)) = \prod_{i=1}^{s} \exp(a_i \tau L_T)\exp(b_i \tau L_U) + O(\tau^{r+1}). \tag{3}$$

Using the Baker–Campbell–Hausdorff (BCH) identity we can find relations that the coefficients a_i, b_i must satisfy to have a high order scheme (Koseleff, 1993, 1996). These are the so-called **order conditions**. For a given set of coefficients a_i, b_i satisfying Eq. 3, the composition

$$z(\tau) = \mathcal{S}(\tau)z(\tau_0) = \prod_{i=1}^{s} \exp(a_i \tau L_T)\exp(b_i \tau L_U)z(\tau_0), \tag{4}$$

is a symplectic map of order r.

The map $\mathcal{S}(\tau)$ is symplectic because it is the product of elementary symplectic maps, $\exp(\tau L_T)$ and $\exp(\tau L_U)$, and has order r because it approximates the exact solution up to order τ^r. We will refer to these kind of symplectic schemes as splitting symplectic integrators.

Some of the main advantages of these kind of integrating schemes are: a) they are very easy to implement; b) they preserve the symplectic character of the Hamiltonian system; and c) in general there is no systematic drift on the conservation of the energy during the numerical integration.

These kind of symplectic schemes have been widely studied throughout the years by several authors (see Hairer et al (2006); McLachlan and Quispel (2002) and references therein). As a matter of fact, splitting methods have been designed (often independently) and extensively used in fields as diverse as molecular dynamics, simulations of storage rings in particle accelerators, quantum chemistry and, of course, celestial mechanics.

There are several procedures to get the order conditions for the coefficients of the splitting scheme in Eq. 4. These are, generally speaking, large systems of polynomial equations in the coefficients that are obtained from Eq. 3. Two of the most popular are the recursive application of the BCH formula to the composition in Eq. 4, and a generalisation of the theory of rooted trees used in the analysis of RungeKutta methods due to Murua and Sanz-Serna (1999) (see also Hairer et al (2006)). The later procedure, while being more systematic than the former, is however not appropriate for the case splitting methods applied to Hamiltonians of the form $A + \epsilon B$. In Blanes et al (2012) a novel systematic way is proposed based on the so-called Lyndon multi-indices that is well adapted to that case.

Splitting methods of order greater than two involve necessarily some negative coefficients a_i and b_j (Goldman and Kaper, 1996; Sheng, 1989; Suzuki, 1991). Although this feature does not imply in principle any special impediment for the class of systems considered in this paper, it is clear that the presence of negative coefficients may affect the numerical error and the maximal step size of the scheme. For this reason, when dealing with high order methods, minimising the size of the negative coefficients and the sum of the absolute value of all the coefficients will be a critical factor in the choice of one particular set of coefficients.

In this paper we do not intend to give the details on the derivation of the order conditions or how to find these coefficients. All these issues are analysed in detail

in Blanes et al (2012). Our aim here is to compare the performance of different splitting symplectic schemes for the specific case of the integration of the Solar System.

If we focus on the motion of the Solar System, or other planetary systems, we have a main massive body in the centre (the Sun) and the other bodies evolve around the centre mass following almost Keplerian orbits. We can take advantage of this to build more efficient schemes. Using an appropriate change of coordinates we can rewrite the Hamiltonian as, $H = H_K + H_I$ (where $|H_I| \ll |H_K|$), a sum of the Keplerian motion of each planet around the central star and a small perturbation due to the interaction between the planets, where H_K and H_I are integrable.

Wisdom and Holman (1991); Kinoshita et al (1991) where the first to split the Hamiltonian of the N-body problem in this way for numerical simulations of the Solar System, by means of what is called a mixed variable integrator, using elliptical coordinates to integrate the Keplerian motion. Splitting the Hamiltonian as $H_K + H_I$ rather than the classical $T(p)+U(q)$ already improves the performance of the leapfrog scheme. As $|H_I|$ is small with respect to $|H_K|$, the system falls into the class of Hamiltonian such that $H = H_A + \varepsilon H_B$ for ε small. In this particular case, the truncation order of the leapfrog scheme is no longer $C\tau^3$ as for $T(p)+U(q)$, but rather $C'\varepsilon\tau^3$ (McLachlan, 1995; Laskar and Robutel, 2001).

In Sections 5 and 6 we will describe different families of symplectic splitting methods for Hamiltonian systems of the kind $H_A + \varepsilon H_B$ and we will compare their performance for the particular case of the Solar System dynamics.

3 The N-Body Problem

Throughout this article we consider the non-relativistic gravitational N-body problem as a test model for the different integrating schemes. We are aware that to have a realistic model for the Solar System dynamics one must include effects like general relativity or tidal dissipation. Nevertheless, and for the sake of simplicity, in this paper these effects are ignored as their presence should not compromise the performance of the schemes presented here.

In a general framework, we consider the motion of $n+1$ particles: the Sun and n planets, that are only affected by their mutual gravitational interaction. Let $\mathbf{u_0}, \mathbf{u_1}, \ldots, \mathbf{u_n}$ and $\dot{\mathbf{u}}_\mathbf{0}, \dot{\mathbf{u}}_\mathbf{1}, \ldots, \dot{\mathbf{u}}_\mathbf{n}$ be the position and velocities, in a barycentric reference frame, of the $n+1$ bodies and let $m_0, m_1, \ldots, m_n$ be their respective masses. For simplicity, we consider m_0 to be the mass of the Sun and m_i for $i = 1, \ldots, n$ the mass of the other planets.

Taking the conjugated momenta $\tilde{\mathbf{u}}_\mathbf{i} = m_i \dot{\mathbf{u}}_\mathbf{i}$, the equations of motion are Hamiltonian, with:

$$H = \frac{1}{2} \sum_{i=0}^{n} \frac{||\tilde{\mathbf{u}}_\mathbf{i}||^2}{m_i} - G \sum_{0 \le i < j \le n} \frac{m_i m_j}{||\mathbf{u_i} - \mathbf{u_j}||}. \tag{5}$$

In this set of coordinates the Hamiltonian naturally splits into, $H = T + U$, where T depends only on the momenta $(\tilde{\mathbf{u}}_\mathbf{i})$ and U depends only on the positions $(\mathbf{u_i})$.

In general, when we deal with complex dynamical systems, it is important to take into account the relevant aspects of the system and use them to build efficient numerical tools to describe their dynamics. In the case of the Solar System we have

a massive body in the centre and the planets evolve following Keplerian orbits around it that vary through time due to their mutual interaction.

Using an appropriate change of variables the Hamiltonian can be written as $H_K + H_I$, where $|H_I|$ is small with respect to $|H_K|$, and both parts are integrable when we considered them on their own. There exist two canonical set of coordinates that allow us to split the Hamiltonian in this way: Jacobi and Heliocentric coordinates.

3.1 Jacobi Coordinates

The Jacobi set of coordinates have been widely used in Celestial Mechanics for developing analytical theories for the planetary motion. They where first used for the numerical integration of the Solar System by Wisdom and Holman (1991).

Here the position of each planet, $\mathbf{v_i}$ for $i = 1, \ldots, n$, is considered relative to the barycentre $\mathbf{G_{i-1}}$ of the previous i bodies, $\mathbf{u_0}, \ldots, \mathbf{u_{i-1}}$, and $\mathbf{v_0}$ is taken as the centre of mass of the system:

$$\left.\begin{aligned} \mathbf{v_0} &= (m_0\mathbf{u_0} + \cdots + m_n\mathbf{u_n})/\eta_n \\ \mathbf{v_i} &= \mathbf{u_i} - (\textstyle\sum_{j=0}^{i-1} m_j\mathbf{u_j})/\eta_{i-1} \end{aligned}\right\}, \tag{6}$$

where $\eta_i = \sum_{j=0}^{i} m_j$. To have a canonical change of variables the momenta $\tilde{\mathbf{v}}_\mathbf{i}$ for $i = 0, \ldots, n$, must be:

$$\left.\begin{aligned} \tilde{\mathbf{v}}_\mathbf{0} &= \tilde{\mathbf{u}}_\mathbf{0} + \cdots + \tilde{\mathbf{u}}_\mathbf{n} \\ \tilde{\mathbf{v}}_\mathbf{i} &= (\eta_{i-1}\tilde{\mathbf{u}}_\mathbf{i} - m_i \textstyle\sum_{j=0}^{i-1} \tilde{\mathbf{u}}_\mathbf{j})/\eta_i \end{aligned}\right\}. \tag{7}$$

In this set of coordinates the Hamiltonian in Eq. 5 takes the form (Laskar, 1990b):

$$\begin{aligned} H_{Jb} = &\sum_{i=1}^{n} \left(\frac{1}{2}\frac{\eta_i}{\eta_{i-1}}\frac{||\tilde{\mathbf{v}}_\mathbf{i}||^2}{m_i} - G\frac{m_i\eta_{i-1}}{||\mathbf{v_i}||} \right) \\ &+ G\left[\sum_{i=2}^{n} m_i \left(\frac{\eta_{i-1}}{||\mathbf{v_i}||} - \frac{m_0}{||\mathbf{r_i}||} \right) - \sum_{0<i<j\leq n} \frac{m_i m_j}{\Delta_{ij}} \right], \end{aligned} \tag{8}$$

where $\Delta_{i,j} = ||\mathbf{u_i} - \mathbf{u_j}||$ (the distance between the two bodies) can be expressed as a function of $\mathbf{v_i}$ and $\mathbf{v_j}$, and $\mathbf{r_i} = \mathbf{u_i} - \mathbf{u_0}$. If we fix the centre of mass at the origin then $\mathbf{v_0} = \mathbf{0}$ and $\tilde{\mathbf{v}}_\mathbf{0} = \mathbf{0}$, and we reduce in 6 the number of equations of motion.

3.2 Heliocentric Coordinates

Here we consider the relative position of each planet with respect to the Sun:

$$\left.\begin{aligned} \mathbf{r_0} &= \mathbf{u_0} \\ \mathbf{r_i} &= \mathbf{u_i} - \mathbf{u_0} \end{aligned}\right\}, \tag{9}$$

and to have a canonical change of variables the momenta are:

$$\left.\begin{aligned} \tilde{\mathbf{r}}_\mathbf{0} &= \tilde{\mathbf{u}}_\mathbf{0} + \cdots + \tilde{\mathbf{u}}_\mathbf{n} \\ \tilde{\mathbf{r}}_\mathbf{i} &= \tilde{\mathbf{u}}_\mathbf{i} \end{aligned}\right\}. \tag{10}$$

In this set of coordinates the Hamiltonian in Eq. 5 takes the form (Laskar, 1990b):

$$H_{He} = \sum_{i=1}^{n} \left(\frac{1}{2} ||\tilde{\mathbf{r}}_\mathbf{i}||^2 \left[\frac{m_0 + m_i}{m_0 m_i} \right] - G \frac{m_0 m_i}{||\mathbf{r_i}||} \right) + \sum_{0<i<j\leq n} \left(\frac{\tilde{\mathbf{r}}_\mathbf{i} \cdot \tilde{\mathbf{r}}_\mathbf{j}}{m_0} - G \frac{m_i m_j}{\Delta_{ij}} \right), \quad (11)$$

where $\Delta_{i,j} = ||\mathbf{r_i} - \mathbf{r_j}||$ for $i, j > 0$. If we consider the centre of mass of the system to be fixed at the origin we have that $\tilde{\mathbf{r}}_\mathbf{0} = 0$, and we can easily recompute $\mathbf{r_0}$ at all time. Hence, we have also reduced in 6 the number of equations of motion.

One of the main differences between these two sets of coordinates is the size of the perturbation which in the case of Jacobi coordinates is smaller than for Heliocentric coordinates (see Table 1 in Section 4).

Moreover, in the case of Jacobi coordinates the perturbation part (H_I) depends only on positions so it is integrable when we consider it alone. But the expressions are more cumbersome than for Heliocentric coordinates (see Appendix B). While in the case of Heliocentric coordinates the perturbation part depends on both position and velocities, hence it is not integrable on its own. In Section 6 we will show how to adapt the splitting schemes to this particular case.

4 Test to Perform

Let $S(\tau) = \prod_{i=1}^{s} \exp(a_i \tau A) \exp(b_i \tau B)$ be a splitting symplectic scheme. We say $S(\tau)$ has s **stages** if it requires s evaluations of $\exp(\tau A) \exp(\tau B)$ per step-size. The smaller the step-size τ used, the smaller is the error of the numerical solution provided by the scheme, and the larger is the computational cost, as more evaluations of $\exp(\tau A) \exp(\tau B)$ are required to integrate over the same time period.

Usually, the higher the order of the scheme the more number s of stages it requires, increasing the computational cost to advance a given step-size τ. So a method with 4 stages will be more efficient than one with 2 stages if it can integrate a given accuracy with a step-size which is at least two times larger than the one required for the 2 stages scheme. In this sense, we define the inverse cost of $S(\tau)$ as τ/s, where s is the number of stages and τ is the step-size used. Thus, if one scheme achieves the same precision than another scheme with smaller inverse cost, then we can say that the former is more efficient than the later.

It is known that, for sufficiently small step-sizes τ, the method $S(\tau)$ integrates exactly (up to exponentially small errors that are below machine accuracy) a modified Hamiltonian system that is close to the original one. Measuring the maximum variation of the energy along a given orbit will gives us a good idea of how close is that modified Hamiltonian to the original Hamiltonian.

Motivated by that, in all our numerical test, we measure the relative precision of a given scheme applied with a given step-size τ by computing the maximum variation ($E_i = \max\{|H(t_0) - H(t)|\}$) of the energy along a given numerical orbit obtained over 10^5 steps of the method (with the same initial conditions at the initial time t_0) and plot the E_i versus the inverse cost τ/s. To fix criteria we will always consider step-sizes of the form: $\tau_i = 1/2^i$ for $i = 0, \ldots, N$.

We are interested in very precise integrations of the Solar System, hence the main goal is to determine for each scheme the maximum step-size (τ_i) required to have an error in the energy variation up to machine accuracy.

Through the paper we consider three test models that we believe illustrate different particularities of the Solar System and can be extrapolated to other planetary systems. These are: a) the motion of the four inner planets (Mercury to Mars); b) the motion of the four outer planets (Jupiter to Neptune) and c) the motion of the eight planets on the Solar System (Mercury to Neptune). The initial conditions and mass parameters have been taken from the JPL Solar System ephemerides DEA405 (`http://ssd.jpl.nasa.gov/`).

Table 1 shows estimates on the size of the perturbation for these three examples for both set of coordinates Jacobi and Heliocentric. To estimate the size of the perturbation we have integrated each system over 100 years and computed the maximum values for $|H_I|$ and $|H_K|$ along this integration. Here `HKep` represents the size of the Keplerian part and `H1max` the size of the perturbation part and the estimated size of the perturbation is given by $\varepsilon =$ `H1max/HKep`.

Table 1 Size of the perturbation in Jacobi and Heliocentric coordinates for the three test examples considered in this work: 4 inner planets (Mercury to Mars), first line; 4 outer planets (Jupiter to Neptune), middle line; 8 planets on the Solar system (Mercury to Neptune), third line.

Jacobi Coord.			Heliocentric Coord.		
HKep	H1max	ε	HKep	H1max	ε
1.3945E-04	6.3342E-10	4.5420E-06	1.3945E-04	9.1652E-10	6.5720E-06
4.2924E-03	8.7162E-07	2.0306E-04	4.2920E-03	2.7184E-06	6.3336E-04
4.4319E-03	8.7158E-07	1.9666E-04	4.4314E-03	2.8042E-06	6.3281E-04

We note that all the simulations in this article have been done using an extended real arithmetics and that we use the compensated summation during the intermediate evaluation of $\exp(a_i\tau A)$ and $\exp(b_i\tau B)$ (see Appendix A).

5 Splitting Symplectic Integrators for Jacobi Coordinates

In Section 3 we have seen that with an appropriate change of variables we can rewrite the Hamiltonian of the N-body planetary system as $H_K + H_I$ where $|H_I| \ll |H_K|$. Hence, the system falls into the class of Hamiltonian that can be expressed as

$$H = H_A + \varepsilon H_B, \tag{12}$$

with $|\varepsilon| \ll 1$. We can take advantage of this to build efficient high-order splitting symplectic integrators (McLachlan, 1995; Laskar and Robutel, 2001). In this section we summarise the main ideas behind these methods and review some of the most relevant schemes.

Using the Lie formalism the formal solution of Eq. (12) is:

$$z(\tau) = \exp[\tau(A + \varepsilon B)]z(\tau_0), \tag{13}$$

where to simplify notation we use $A \equiv \{H_A, \cdot\} = L_{H_A}$, $B \equiv \{H_B, \cdot\} = L_{H_B}$. We recall that H_A and H_B are integrable, hence we can compute explicitly $\exp(\tau A)$

and $\exp(\tau\varepsilon B)$. To have a splitting symplectic integrator of order r, we need to find the coefficients a_i, b_i such that

$$\mathcal{S}_r(\tau) = \prod_{i=1}^{s} \exp(a_i \tau A) \exp(\varepsilon b_i \tau B), \tag{14}$$

satisfies $|\mathcal{S}_r(\tau) - \exp[\tau(A+\varepsilon B)]| = \mathcal{O}(\tau^{r+1})$. The Baker–Campbell–Hausdorff (BCH) theorem ensures us that $\mathcal{S}_r(\tau) = \exp(\tau\mathcal{H})$, where $\mathcal{H}$ is also a Hamiltonian system and belongs to the free Lie algebra generated by A and B, $\mathcal{L}(A,B)$. Moreover, we can express $\mathcal{H}$ as a double asymptotic series in τ and ε:

$$\begin{aligned} \tau\mathcal{H} = \; & \tau p_{1,0} A \; + \; \varepsilon\tau p_{1,1} B \; + \; \varepsilon\tau^2 p_{2,1}[A,B] + \varepsilon\tau^3 p_{3,1}[[A,B],A] \\ & + \; \varepsilon^2\tau^3 p_{3,2}[[A,B],B] \; + \; \varepsilon\tau^4 p_{4,1}[[[A,B],A],A] \\ & + \; \varepsilon^2\tau^4 p_{4,2}[[[A,B],B],A] \; + \; \varepsilon^3\tau^4 p_{4,3}[[[A,B],B],B] \; + \; \ldots, \end{aligned} \tag{15}$$

where $p_{i,j}$ are polynomials in a_k and b_k.

To have a symplectic scheme of order r we need:

$$\begin{aligned} p_{1,0} &= a_1 \; + \; a_2 \; + \; \cdots \; + \; a_s = 1, \\ p_{1,1} &= b_1 \; + \; b_2 \; + \; \cdots \; + \; b_s = 1, \\ p_{i,j} &= 0, \; \forall i,j \leq r. \end{aligned}$$

The scheme $\mathcal{S}_r(\tau)$ is symmetric if it verifies $\mathcal{S}_r^{-1}(\tau) = \mathcal{S}_r(-\tau)$, in which case all the even terms in τ in Eq. 15 vanish, having less conditions to satisfy for a scheme of a given order, r, enabling us to find high-order schemes at lower computational cost. There are two different types of symmetric compositions (Eq. 14): one in which the first and last exponentials correspond to the A part (and thus called $\mathcal{ABA}$ composition),

$$\mathcal{ABA}: \quad \mathrm{e}^{a_1\tau A}\,\mathrm{e}^{\varepsilon b_1\tau B}\,\mathrm{e}^{a_2\tau A}\,\cdots\,\mathrm{e}^{a_2\tau A}\,\mathrm{e}^{\varepsilon b_1\tau B}\,\mathrm{e}^{a_1\tau A} \tag{16}$$

and the other in which the role of $\exp(\tau A)$ and $\exp(\varepsilon\tau B)$ is interchanged ($\mathcal{BAB}$ composition):

$$\mathcal{BAB}: \quad \mathrm{e}^{\varepsilon b_1\tau B}\,\mathrm{e}^{a_1\tau A}\,\mathrm{e}^{\varepsilon b_2\tau B}\,\cdots\,\mathrm{e}^{\varepsilon b_2\tau B}\,\mathrm{e}^{a_1\tau A}\,\mathrm{e}^{\varepsilon b_1\tau B}. \tag{17}$$

All the integration schemes that we present in this paper correspond to the $\mathcal{ABA}$ class. For the experiments carried out, we have not found substantial differences in the efficiency with respect to methods in the $\mathcal{BAB}$ class.

Notice that for symmetric methods, the last exponential at one step can be concatenated with the first one at the next integration step when the method is iterated, so the number of exponentials $\exp(\tau A)$ and $\exp(\varepsilon\tau B)$ per step is s, the number of stages.

It is clear that in many cases $|\varepsilon| \ll \tau$ (or at least $\varepsilon \approx \tau$). So we can have high-order schemes by only killing the error terms with small powers of ε, and save computational cost by decreasing the number of stages of the method.

Depending of the nature of the problem we can try to find the appropriate terms in $\varepsilon^i\tau^p$ that must vanish in order to have an optimal performance. For example,

if we consider a method such that the coefficients a_i, b_i satisfy $p_{1,0} = p_{1,1} = 1$ and $p_{2,1} = p_{3,1} = p_{4,1} = 0$, then,

$$|\mathcal{H} - (A + \varepsilon B)| = \mathcal{O}(\varepsilon\tau^4 + \varepsilon^2\tau^2),$$

but as $|\varepsilon| \ll \tau$ this method is of effective order 4. In a more general context we will have methods such that,

$$|\mathcal{H} - (A + \varepsilon B)| = \mathcal{O}(\varepsilon\tau^{s_1} + \varepsilon^2\tau^{s_2} + \varepsilon^3\tau^{s_3} + \cdots + \varepsilon^m\tau^{s_m}). \tag{18}$$

We remark that s_1 is the error of consistency for the scheme, i.e. is the error behaviour in the limit case $\varepsilon \to 0$. Nevertheless, in many cases for small step-sizes the method can behave as one of order s_2. In what follows we will refer to the generalised order of a method in terms of the order in powers of ε. Hence, we will say that a method has order (s_1, s_2) if $|\mathcal{H} - (A + \varepsilon B)| = \mathcal{O}(\varepsilon\tau^{s_1} + \varepsilon^2\tau^{s_2})$. In terms of the local error, we have $|\mathcal{S}(\tau) - \exp[\tau(A + \varepsilon B)]| = \mathcal{O}(\varepsilon\tau^{s_1+1} + \varepsilon^2\tau^{s_2+1})$.

5.1 $\mathcal{ABA}$ schemes of generalised order $(2n, 2)$

McLachlan (1995) noted that as $|\varepsilon| \ll \tau$ we can have high-order methods by only killing the terms in $\varepsilon\tau^k$. Independently Chambers and Murison (2000); Laskar and Robutel (2001) dealt with this problem following similar ideas, (Laskar and Robutel, 2001) providing an explicit computation of the coefficients of the remainder for all order k. One of the main advantages of only killing the terms in $\varepsilon\tau^k$ is that we are sure that all the coefficients a_i, b_i will be positive. As a consequence the coefficients a_i, b_i will be small and the numerical scheme will be stable.

In Table 2 we summarise the coefficients for the different $\mathcal{ABA}$ $(2n, 2)$ schemes for $n = 1, \ldots, 4$. For further details on how to find the a_i, b_i coefficients and the coefficients for $n \geq 4$ see (McLachlan, 1995; Laskar and Robutel, 2001). Since all the methods we consider are symmetric, we only collect the necessary coefficients of each scheme. Thus, $\mathcal{ABA}(8, 2)$ corresponds to the composition

$$\mathrm{e}^{a_1\tau A}\,\mathrm{e}^{b_1\varepsilon\tau B}\,\mathrm{e}^{a_2\tau A}\,\mathrm{e}^{b_2\varepsilon\tau B}\,\mathrm{e}^{a_3\tau A}\,\mathrm{e}^{b_2\varepsilon\tau B}\,\mathrm{e}^{a_2\tau A}\,\mathrm{e}^{b_1\varepsilon\tau B}\,\mathrm{e}^{a_1\tau A}.$$

We will follow this convention throughout the text.

In Figure 1 we compare the performance of the $\mathcal{ABA}(2n, 2)$ for $n = 1, 2, 3, 4$ for the 4 inner planets (left) and the 4 outer planets (right). The x-axis corresponds to the cost of the scheme (τ/s) and the y-axis corresponds to the maximum energy variation for one integration at constant step-size τ. Laskar and Robutel (2001) already saw that the optimal schemes for this problem where those of orders $(6, 2)$ and $(8, 2)$ (i.e. $\mathcal{SABA}_3$ and $\mathcal{SABA}_4$ following their notation).

The error on the Hamiltonian approximation of these schemes is $\mathcal{O}(\varepsilon\tau^{2n}+\varepsilon^2\tau^2)$. In Figure 1 we can see how the error in energy decreases in τ with slope $2n$ for large steps-sizes and slope 2 for smaller steps-sizes. We also see how for small step-sizes there is no difference between the cost of the $\mathcal{ABA}62$ and $\mathcal{ABA}82$ schemes. In order to improve their performance we need to kill the term in $\varepsilon^2\tau^2$ rather than those of order $\varepsilon\tau^{2k}$ for $k > 4$, which are the limiting factor of these schemes.

Table 2 Coefficients for the $\mathcal{ABA}(2n,2)$ methods for $n = 1,\ldots,4$ (Laskar and Robutel, 2001).

id	order	stages	a_i, b_i		
ABA22	$(2,2)$	1	a_1	$=$	$1/2$
			b_1	$=$	1
ABA42	$(4,2)$	2	a_1	$=$	$1/2 - \sqrt{3}/6$
			a_2	$=$	$\sqrt{3/3}$
			b_1	$=$	$1/2$
ABA62	$(6,2)$	3	a_1	$=$	$1/2 - \sqrt{15}/10$
			a_2	$=$	$\sqrt{15}/10$
			b_1	$=$	$5/18$
			b_2	$=$	$4/9$
ABA82	$(8,2)$	4	a_1	$=$	$1/2 - \sqrt{525+70\sqrt{30}}/70$
			a_2	$=$	$\left(\sqrt{525+70\sqrt{30}} - \sqrt{525-70\sqrt{30}}\right)/70$
			a_3	$=$	$\sqrt{525-70\sqrt{30}}/35$
			b_1	$=$	$1/4 - \sqrt{30}/72$
			b_2	$=$	$1/4 + \sqrt{30}/72$

5.2 $\mathcal{ABA}$ schemes of order $(2n,4)$

In this section we will describe three different procedures to cancel the dominant term $\varepsilon^2\tau^2$ in order to get methods of generalized order $(2n,4)$, and discuss their performance for the different test models described in Section 4.

5.2.1 The corrector term ($\mathcal{SC}$)

Since in Jacobi coordinates A is quadratic in p and B depends only of q, then it follows that the term $[[A,B],B]$ depends only on q and thus $\exp(\tau^3\varepsilon^2[[A,B],B])$ can be easily computed. Laskar and Robutel (2001) noticed that it is possible to incorporate this term into the previous compositions with a conveniently chosen constant so as to cancel the term of order $\varepsilon^2\tau^2$ in the asymptotic expansion Eq. 15. We note that this corrector scheme is different than the one introduced by Wisdom et al (1996) where the corrector added at the beginning and at the end of each step-size is a change of variables.

Thus, let $\mathcal{S}_n(\tau)$ be one of the symplectic $\mathcal{ABA}$ schemes of order $(2n,2)$ described in Section 5.1. We can get rid of the term in $\varepsilon^2\tau^2$ by considering

$$\mathcal{SC}_n(\tau) = \exp\left(-\tau^3\varepsilon^2\frac{c}{2}[[A,B],B]\right)\ \mathcal{S}_n(\tau)\ \exp\left(-\tau^3\varepsilon^2\frac{c}{2}[[A,B],B]\right), \qquad (19)$$

with the appropriate choice of the constant c. In Table 3 we show the value for the coefficient c for each the four $\mathcal{ABA}(2n,2)$ schemes described before. For further details see (Laskar and Robutel, 2001). Notice that $\mathcal{SC}_n$ corresponds to integrating $\log(\mathcal{S}_n(\tau))\ -\tau^3\varepsilon^2 cL_{\{\{A,B\},B\}}$ using the leapfrog scheme.

So using Eq. 19 with any of the $\mathcal{ABA}$ $(2n,2)$ scheme in Section 5.1 we obtain a new integrating scheme of order $(2n,4)$ with no negative intermediate step.

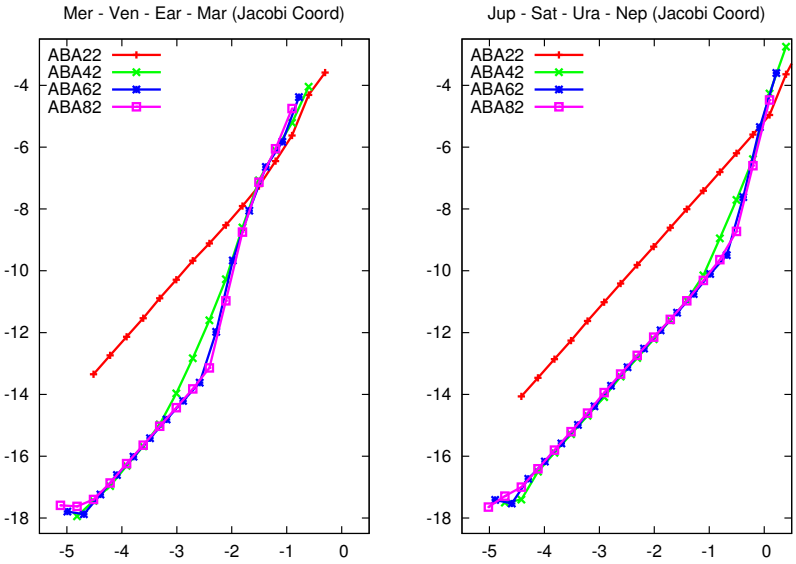

Fig. 1 Comparison between the $\mathcal{ABA}(2n,2)$ methods for $n=1,2,3,4$ applied to the 4 inner planets (left) and the 4 outer planets (right). The x-axis represents the cost (τ/s) and the y-axis is the maximum energy variation over one integration with constant step-size τ. Here s is the number of stages.

Table 3 Coefficients c for the corrector term applied to the $\mathcal{ABA}(2n,2)$ schemes in Table 2 (Laskar and Robutel, 2001).

`order`	c
1	$1/12$
2	$(2-\sqrt{3})/24$
3	$(54-13\sqrt{15})/648$
4	0.00339677504820860133153215778349214 4

5.2.2 The composition scheme ($\mathcal{S}2^m$)

Yoshida (1990) and Suzuki (1990) independently came up with the same idea to find a symmetric scheme of order $2k+2$ from one of order $2k$. They both noticed that if $\mathcal{S}(\tau)$ is a scheme of order $2k$, then:

$$\mathcal{S}2k(\tau)=\mathcal{S}(x_0\tau)\mathcal{S}(x_1\tau)\mathcal{S}(x_0\tau), \tag{20}$$

is a scheme of order $2k+2$ for an appropriate choice of the constant coefficients x_0,x_1. One can check that x_0,x_1 must satisfy $2x_0+x_1=1$ and $2x_0^{2k+1}+x_1^{2k+1}=0$. Notice that the second condition is used to cancel all the terms of order $2k$, while the first one is only for consistency.

Laskar and Robutel (2001) used this idea to turn any of the $\mathcal{ABA}$ schemes of order $(2n,2)$ into one of order $(2n,4)$. If $\mathcal{S}(\tau)$ is a symmetric $\mathcal{ABA}$ scheme of order (2n,2) then the composition:

$$\mathcal{S}2^m(\tau)=\mathcal{S}^m(y_0\tau)\mathcal{S}(y_1\tau)\mathcal{S}^m(y_0\tau). \tag{21}$$

is a symmetric method of order $(2n, 4)$ if y_0, y_1 satisfy $2my_0 + y_1 = 1$ and $2my_0^3 + y_1^3 = 0$ so, $(y_0 = 1/(2m - (2m)^{1/3}),\ y_1 = -(2m)^{1/3}/(2m - (2m)^{1/3}))$.

We have done several test to determine the optimal value of m, and our test show that this one is given by $m = 2$. These results are consistent with those of (Suzuki, 1990; McLachlan, 2002) who did a similar study in a more general framework. The main advantage of this scheme is that we can use it for both Heliocentric and Jacobi coordinates.

5.2.3 McLachlan extra stage scheme ($\mathcal{ABA}84$)

McLachlan (1995) studied the possibility of adding an extra stage to the $\mathcal{ABA}(2n, 2)$ schemes to get rid of the $\varepsilon^2\tau^2$ term. To add an extra stage derives into having an extra pair of coefficients a_i, b_i and an extra algebraic equation to satisfy. All the coefficients will no longer be positive (Suzuki, 1991). In general, if the coefficients are not very large, these methods are stable. The coefficients for the $\mathcal{ABA}$ method of generalised order $(8, 4)$ provided by McLachlan (1995) are summarised in Table 4.

Table 4 Coefficients for the $\mathcal{ABA}$ method of order $(8, 4)$ found by (McLachlan, 1995).

id	order	stages	a_i, b_i		
ABA84	$(8, 4)$	5	a_1	=	0.075346960269892888841652780368
			a_2	=	0.517916854688256782300773978 50
			a_3	=	-0.093263814958149670717301782 18
			b_1	=	0.190225939373676619245230762 74
			b_2	=	0.846524070443526257055080544 65
			b_3	=	-1.073500019634405752600622614 77

5.2.4 Results

In Figure 2 we compare the performance of these three different approaches to build methods of generalised order (8,4) against the $\mathcal{ABA}82$ scheme. In the plots we show the cost (τ/s) vs the maximum energy variation for the three test models: the 4 inner planets (left), the 4 outer planets (middle) and the 8 planets in the Solar System (right).

As we can see, the three different schemes improve considerably the performance of the $\mathcal{ABA}82$ (red line). In all cases the corrector scheme $\mathcal{SC}$ (blue line) and the McLachlan $\mathcal{ABA}84$ (purple line) show a similar quantitative behaviour. The difference between them is the cost of the extra stage in $\mathcal{ABA}84$, as we are assuming that the corrector is completely free. We note that this is not entirely true if the number of bodies is large $(n \geq 4)$. On the other hand, the composition methods, $\mathcal{S}\in^m$ (green line), improves the performance with respect to the $\mathcal{ABA}82$ (red line) but is much more expensive than the other two schemes.

5.3 $\mathcal{ABA}$ schemes with generalised order $(s_1, s_2, \dots)$

In the previous section we have seen that adding an extra stage to cancel the term of order $\varepsilon^2\tau^2$ gives good results. We can extend this idea and add more stages to

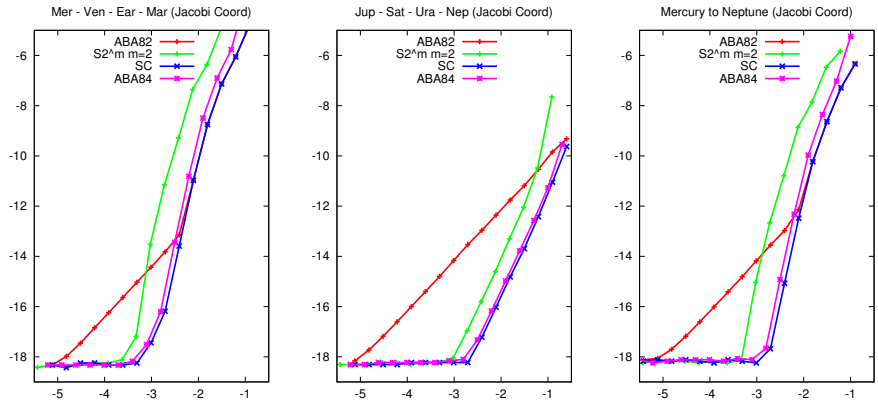

Fig. 2 Comparison between the different schemes to kill the the $\varepsilon^2\tau^2$ terms in the $\mathcal{ABA}82$ scheme. From left to right: the 4 inner planets, the 4 outer planets and the whole Solar System. The x-axis represents the cost (τ/s) and the y-axis the maximum energy variation for one integration with constant step-size τ.

kill the error terms accounting to the main limiting factor for each problem (Blanes et al, 2012). This translates into adding more constraints on the coefficients. As long as the increase in the computational cost is less than the gain in accuracy these methods will be competitive. In Figure 2 we see that the dominant error term for the $\mathcal{ABA}84$ varies between the different test models. Notice that for the outer planetary system the scheme behaves as one of order 4, so the dominant term is $\varepsilon^2\tau^4$. On the other hand, for the inner planetary system, the method behaves as one of order 8, now the dominant term is $\varepsilon\tau^8$.

Hence, to improve the performance of the McLachlan's $\mathcal{ABA}84$ we need to kill different error terms depending on the problem. For the inner planets, a method of order $(10, 4)$ should perform better than one of order $(8, 6)$. While for the outer planets a method of order $(8, 6)$ should give better results than one of order $(10, 4)$.

In Blanes et al (2012) we find details on how to solve the algebraic equations and find the set of coefficients a_i, b_i that provide $\mathcal{ABA}$ schemes for a given arbitrary order $(s_1, s_2, \dots)$. We must mention that there is no unique combination of coefficients a_i, b_i for a given order. From all the possible solutions we have selected those that give a better approximation and whose coefficients a_i, b_i are small. In Table 5 we summarise the coefficients for three $\mathcal{ABA}$ schemes: one of order $(10, 4)$; one of order $(8, 6, 4)$ and one of order $(10, 6, 4)$.

5.3.1 Results

In Figure 3 we compare the performance of the three schemes summarised in Table 5 against the $\mathcal{ABA}82$ and $\mathcal{ABA}84$ for the three test models.

In the left-hand side of Figures 3 we have the results for the 4 inner planets. We recall that the dominant error term in the $\mathcal{ABA}84$ scheme was $\varepsilon\tau^8$. Hence, a method of order 10 in ε should perform better than one of order 8 in ε. Nevertheless, as we can see there is no significant gain in the performance of these schemes with respect to $\mathcal{ABA}84$. Apparently, for these methods the gain in precision is proportional to the computational cost in this range of accuracy.

Table 5 Coefficients for $\mathcal{ABA}$ symmetric splitting methods of orders $(10,4)$, $(8,6,4)$ and $(10,6,4)$ (Blanes et al, 2012).

id	order	stages	a_i, b_i		
ABA104	$(10,4)$	7	a_1	=	0.047067100645972506129478876372
			a_2	=	0.184756935417088106924737619370
			a_3	=	0.282706005679836205324361656554
			a_4	=	-0.014530041742896818378578152296
			b_1	=	0.118881917368197019945350395085
			b_2	=	0.241050460551501565744166786590
			b_3	=	-0.273286666705323806054311398166
			b_4	=	0.826708577571250440729588432981
ABA864	$(8,6,4)$	7	a_1	=	0.071133426498223117777938730006
			a_2	=	0.241153427956640098736487795326
			a_3	=	0.521411761772814789212136078067
			a_4	=	-0.333698616227678005726562603400
			b_1	=	0.183083687472197221961703757166
			b_2	=	0.310782859898574869507522291054
			b_3	=	-0.026564618511958800697212137916
			b_4	=	0.065396142282373418455972179391
ABA1064	$(10,6,4)$	8	a_1	=	0.038094497422412195456975322308
			a_2	=	0.145298716116913749294020072660
			a_3	=	0.207627695725541250716205611324
			a_4	=	0.435909703651526159223154862401
			a_5	=	-0.653861225832786709380711737390
			b_1	=	0.095858880837075210610771503771
			b_2	=	0.204446153142998780680507783916
			b_3	=	0.217070347978991101714338592430
			b_4	=	-0.017375381959065093005617880118

In the middle of Figure 3 we have the results for the 4 outer planets. We recall that here the dominant term in the $\mathcal{ABA}84$ scheme was $\varepsilon^2\tau^4$, hence we expect the schemes of order 6 in ε^2 to be better than the $\mathcal{ABA}84$. As we can see the $\mathcal{ABA}864$ and the $\mathcal{ABA}1064$ schemes give better results that the $\mathcal{ABA}84$. In both cases the optimal cost is around 10^{-2} vs an optimal cost of around 10^{-3} for the $\mathcal{ABA}84$ scheme.

The main difference between the inner planets and the outer planets is the size of the perturbation. We recall that in Jacobi coordinates, for the inner planets $\varepsilon \approx 4.54 \cdot 10^{-6}$, while for the outer planets $\varepsilon \approx 2.03 \cdot 10^{-4}$ (see Table 1). The difference of about 2 orders of magnitude should explain the difference in the performance of the different schemes, as the relevance of the terms $\varepsilon^i\tau^{2k}$ in the error approximation will vary depending on the size of ε.

Taking this into account, one can be surprised by the performance of these schemes when we consider the whole Solar System (Figure 3 right). Here the size of the perturbation ($\varepsilon \approx 1.96 \cdot 10^{-4}$) is of the same order of magnitude as the case of the outer planets. But as we can see in Figure 3 the schemes behave in the same way as the case of the inner planets, where the terms of order $\varepsilon\tau^8$ dominate those of order $\varepsilon^2\tau^4$. We think this is due to Mercury: its fast orbital period and large eccentricity is limiting the performance of the methods. This phenomena was already noticed by Wisdom et al (1996) and re-discussed by Viswanath (2002). This is why Saha and Tremaine (1994) proposed to use independent time-steps for

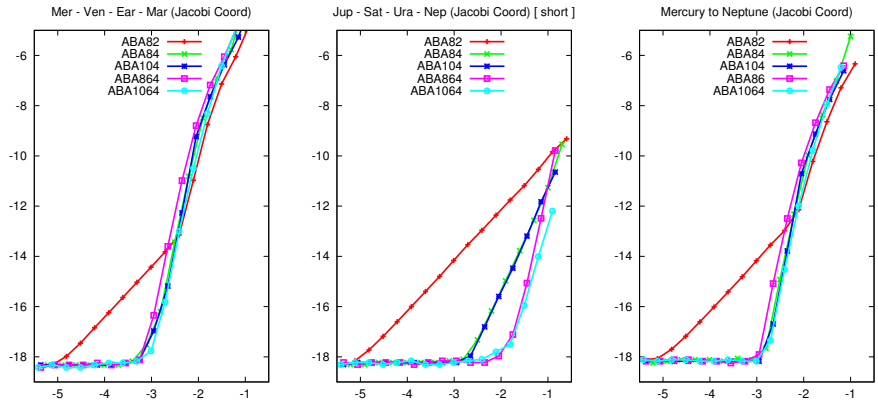

Fig. 3 Comparison between the $\mathcal{ABA}$ splitting schemes of arbitrary order (s_1, s_2, s_3) summarised in Table 5 against the $\mathcal{ABA}82$ and $\mathcal{ABA}84$. From left to right: the 4 inner planets, the 4 outer planets and the whole Solar System. The x-axis represents the cost (τ/s) and the y-axis the maximum energy variation for one integration with constant step-size τ.

each planet. They used the leapfrog scheme and adapted it to take fractions of the given step-size for each planet, depending on their orbital period. It is not trivial to extend these ideas using the higher order schemes described in this section, and a second order method is not the appropriate option to achieve round-off accuracy.

6 Splitting Symplectic Integrators for Heliocentric

We recall that all the tests done in Section 5 have been done using Jacobi coordinates. All these integrating schemes assume that the two parts of the Hamiltonian H_A, H_B are integrable. This is true for Jacobi coordinates where:

$$H_{Jb}(q,p) = H_K(q,p) + H_I(q). \tag{22}$$

where $H_K(q,p)$ is integrable (it is a sum of independent Kepler problems) as well as $H_I(q)$ (it only depends on q). However, this is not true for Heliocentric coordinates where:

$$H_{He}(q,p) = H_K(q,p) + H_I(q,p), \tag{23}$$

and $H_I(q,p)$ is not integrable, which can be a problem if we want to apply the splitting schemes presented in Section 5.

An option to deal with the non-integrability of $H_I(q,p)$ is to use another numerical method to integrate $H_I(q,p)$ and compute the $\exp(b_i\tau B)$ up to machine accuracy. Unfortunately, this can drastically increase the computational cost of the schemes.

We propose to use the fact that $H_I(q,p) = T_1(p) + U_1(q)$ splits naturally into two parts, one depending on positions, the other in velocities. These two parts are integrable on its own and small with respect to $H_K(q,p)$. In a general framework, the Hamiltonian splits as:

$$H = H_A + \varepsilon(H_B + H_C),$$

where H_A, H_B and H_C, are integrated when we consider them separately. In the same way as in Section 5, we could try to find appropriate coefficients a_i, b_i, c_i, such that

$$\mathcal{S}(\tau) = \prod_{i=1}^{s} \exp(a_i \tau A) \exp(\varepsilon b_i \tau B) \exp(\varepsilon c_i \tau C),$$

approximates $\exp(\tau L_H)$. As before, to simplify notation $A \equiv \{H_A, \cdot\}$, $B \equiv \{H_B, \cdot\}$ and $C \equiv \{H_C, \cdot\}$. Then one has to deal with the Lie Algebra generated by A, B and C. The number of order conditions as well as the complexity to solve them numerically to get the coefficients a_i, b_i, c_i grows extraordinarily with the order Blanes et al (2012). A simple alternative way to proceed is to use the splitting symplectic schemes in Section 5:

$$\mathcal{S}(\tau) = \prod_{i=1}^{n} \exp(a_i \tau A) \exp(\varepsilon b_i \tau (B + C)). \tag{24}$$

and approximate $\exp(\varepsilon b_i \tau (B + C))$ with

$$\exp(\varepsilon b_i \tau (B + C)) \approx \exp(\varepsilon \frac{b_i}{2} \tau C) \exp(\varepsilon b_i \tau B) \exp(\varepsilon \frac{b_i}{2} \tau C). \tag{25}$$

Here we take C as the Lie operator associated to $T_1(p)$ due to its lower computational cost.

In general H_B and H_C do not commute ($\{H_B, H_C\} \neq 0$), so this approximation adds an extra error contribution term, $\varepsilon^3 \tau^2$, which will be negligible for small ε. In Figure 4 we see the result of taking the $\mathcal{ABA}82$, the $\mathcal{ABA}84$ and the $\mathcal{S}2^m$ splitting schemes using Eq. 25 to deal with Heliocentric coordinates. We can see that in general the symplectic schemes have the same behaviour as with Jacobi coordinates (Figure 2).

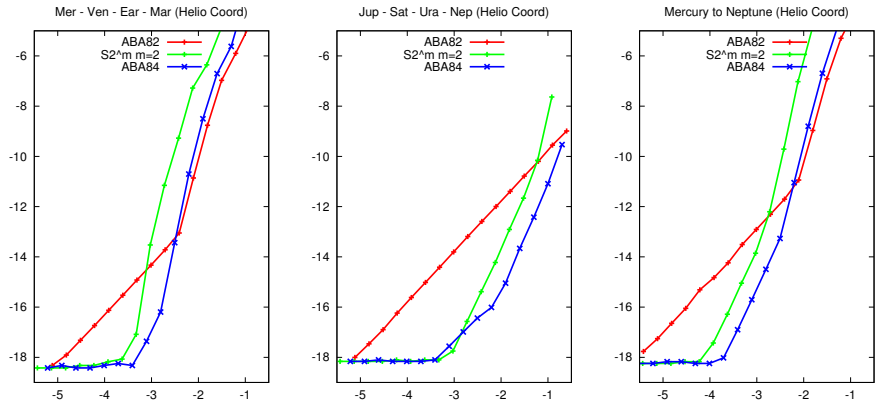

Fig. 4 Comparison between the $\mathcal{ABA}82$, $\mathcal{ABA}84$ and $\mathcal{S}2^m$ schemes discussed in Section 5.2 applied to Heliocentric coordinates. From left to right: the 4 inner planets, the 4 outer planets and the whole Solar System. The x-axis represents the cost (τ/s) and the y-axis the maximum energy variation for one integration with constant step-size τ.

We do see a difference in the case of the outer planets (Figure 4 middle). Now the $\mathcal{ABA}84$ scheme behaves as one of order 2 for small step-sizes. This is due to

the extra error term $\varepsilon^3\tau^2$. We recall that the main difference between the inner and the outer planets is the size of the perturbation (ε) which is smaller in the first case. Here the terms of order $\varepsilon^3\tau^2$ are negligible for the inner planets but not for the outer planets.

Unfortunately, when we consider high-order symplectic schemes like the ones presented in Sections 5.3 these extra error term will become relevant, jeopardising the performance of these schemes.

Chambers (1999); Wisdom (2006) proposed to rewrite the Hamiltonian in Heliocentric variables so that H_B and H_C commuted ($\{H_B, H_C\} = 0$), and then used the fact that $\exp(\varepsilon b_i \tau(B + C)) = \exp(\varepsilon b_i \tau B)\exp(\varepsilon b_i \tau C)$. For further details see Appendix C.

6.1 $\mathcal{ABAH}$ $(2n, 4)$ specific for Heliocentric coordinates

We have just seen that for Heliocentric coordinates we can adapt the splitting schemes described is Section 5 using Eqs. 24 and 25. But with this an extra term $\varepsilon^3\tau^2$ appears in the error approximation that will limit the performance for high-order schemes. One can check that this error terms is associated to the algebraic expression $b_1^3 + b_2^3 + \cdots + b_n^3$. We can add an extra stage to the scheme so that it also satisfies:

$$b_1^3 + b_2^3 + \cdots + b_n^3 = 0,$$

leading to symplectic schemes with the same generalised order as before for Heliocentric coordinates. Table 6 collects the coefficients for the $\mathcal{ABAH}$ scheme of order $(8, 4)$ for Heliocentric coordinates. This scheme has the same effective order as the McLachlan $\mathcal{ABA}$ scheme of order $(8, 4)$ (Section 5.2.3) but it is specific for Heliocentric coordinates. In Figure 5 we compare the performance of this new scheme against the $\mathcal{ABA}$84 scheme. As we can see, for the outer planets the new $\mathcal{ABAH}$844 scheme behaves better that the $\mathcal{ABA}$84 for small step-sizes.

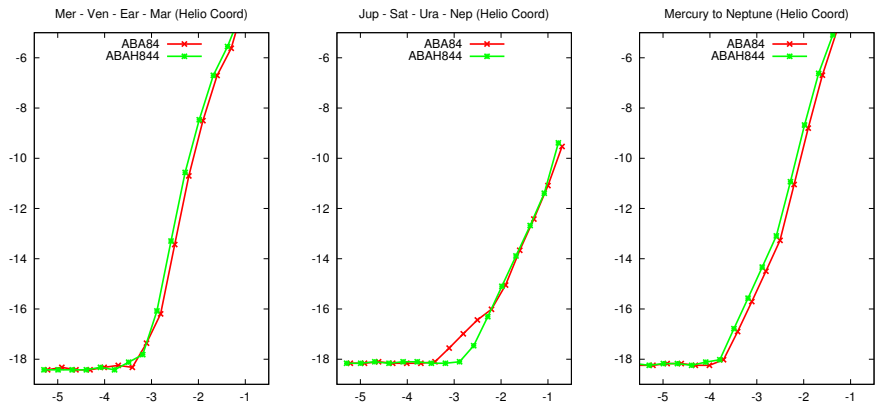

Fig. 5 Comparison between $\mathcal{ABA}$84 and $\mathcal{ABAH}$844. From left to right: the 4 inner planets, the 4 outer planets and the whole Solar System. The x-axis represents the cost (τ/s) and the y-axis the maximum energy variation for one integration with constant step-size τ.

Table 6 Coefficients for $\mathcal{ABAH}$ specific symmetric splitting methods for Heliocentric coordinates of orders (8,4), (8, 6, 4) and (10, 6, 4) (Blanes et al, 2012).

id	order	stages	a_i, b_i		
ABAH844	$(8,4)$	6	a_1	=	0.27414026894340187616405654402
			a_2	=	-0.10756843844016423062511052968
			a_3	=	-0.04801850259060169269119541721
			a_4	=	0.76289334417472809430449880574
			b_1	=	0.64088579516251271773224911649
			b_2	=	-0.85857544895678285658812832469
			b_3	=	0.71768965379427013885587920820
ABAH864	$(8,6,4)$	8	a_1	=	0.06810235651658372084723976682
			a_2	=	0.25113603872210332330728295804
			a_3	=	-0.07507264957216562516006821767
			a_4	=	-0.00954471970174500781148821895
			a_5	=	0.53075794807044717763406742353
			b_1	=	0.16844325936189545343103826977
			b_2	=	0.42431771737426772243003516574
			b_3	=	-0.58581096946817568123090153554
			b_4	=	0.49304999273201250536982810002
ABAH1064	$(10,6,4)$	9	a_1	=	0.04731908697653382270404371796
			a_2	=	0.26511052357487851595394800361
			a_3	=	-0.00997652288381124084326746816
			a_4	=	-0.05992919973494155126395247987
			a_5	=	0.25747611206734045344922822646
			b_1	=	0.11968846245853220353128642974
			b_2	=	0.37529558553793742504201285376
			b_3	=	-0.46845934183259937836508204098
			b_4	=	0.33513973427558970103930989429
			b_5	=	0.27667111912108009750494572633

6.2 $\mathcal{ABAH}$ specific methods with arbitrary order $(s1, s2, ...)$

In the same way we can add the extra constraint $b_1^3 + \cdots + b_n^3 = 0$ to the high-order schemes in Section 5.3 to have high order splitting schemes specific for Heliocentric coordinates. In Table 6 we show the coefficients of two $\mathcal{ABAH}$ schemes of orders $(8, 6, 4)$ and $(10, 6, 4)$. All these schemes have one more stage than the schemes presented in Table 5.

In Figure 6 we compare the performance of the $\mathcal{ABA}82$ with the other three schemes in Table 6. Where the behaviour of the schemes depending on its order is similar to the one presented in Jacobi coordinates. For the inner planets (Figure 6 left) all $\mathcal{ABAH}$ schemes present a similar optimal cost. For the outer planets (Figure 6 middle) the $\mathcal{ABAH}$ schemes of order $(8, 6, 4)$ and $(10, 6, 4)$ are much better than the other two schemes. We recall that here the size of the perturbation is larger and killing the terms of order $\varepsilon^3\tau^4$ does make a difference. Finally, if we consider the 8 planets in the Solar System (Figure 6 right) here the $\mathcal{ABAH}$ schemes of order $(8, 6, 4)$ and $(10, 6, 4)$ do improve the performance of the schemes of order $(8, 4)$. We recall that this was not the case in Jacobi coordinates (Figure 3).

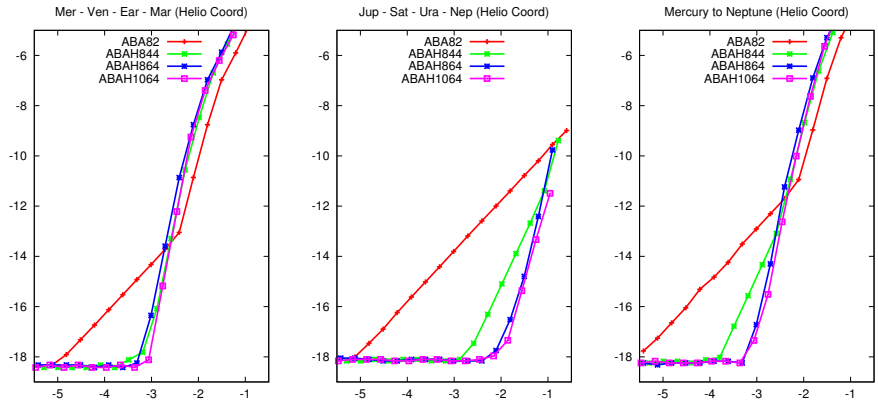

Fig. 6 Comparison between $\mathcal{ABAH}$ schemes of order $(8,4,4)$, $(8,6,4)$ and $(10,6,4)$ specific for Heliocentric coordinates and the $\mathcal{ABA}82$. From left to right: the 4 inner planets, the 4 outer planets and the whole Solar System. The x-axis represents the cost (τ/n) and the y-axis the maximum energy variation for one integration at constant step-size τ.

7 Jacobi vs Heliocentric coordinates

In Sections 5 and 6 we have described different splitting schemes for both Jacobi and Heliocentric set of coordinates. In the case of Heliocentric coordinates the expressions for the Hamiltonian are less cumbersome and easier to handle (see Appendix B). But the size of the perturbation is larger than in Jacobi coordinates and an extra stage to deal with the non-integrability of H_I must be added to have high-order schemes. Here we want to compare the performance of the different schemes for both set of coordinates.

We compare the performance of the $\mathcal{ABA}$ methods of order $(8,2)$, $(8,4)$ and $(10,6,4)$ in both set of coordinates, with the three test models used throughout this report. We recall that the $(8,4)$ and $(10,6,4)$ schemes have an extra stage in Heliocentric coordinates. In Figure 7 we summarise the performance of these schemes. From left to right we have the results for the inner planets, the outer planets and the whole Solar System. We distinguish the order of the schemes by the colour. Where the lines in red represent the schemes of order $(8,2)$, the blue lines those of order $(8,4)$ and the purple lines those of order $(10,6,4)$. We use continuous lines to refer to Jacobi coordinates and discontinuous lines for Heliocentric coordinates.

If we look at the results for the inner planets (Figure 7 left), we can see there is not much difference between taking Jacobi or Heliocentric coordinates (continuous vs discontinuous lines). In both cases the size of the perturbation is small (Table 1) and there is not much difference between taking a splitting scheme of order $(8,4)$ or $(10,6,4)$. In both cases the terms in ε in the error expansion are the ones that matter, but there is not much difference between taking order 8 or 10 in $\varepsilon\tau^k$. We should have to use arithmetics with higher precision to see the difference (see Appendix D). Hence the $\mathcal{ABA}84$ is the best choice for this case.

If we look at the results for the outer planets (Figure 7 middle), again there is no significant difference between Jacobi and Heliocentric coordinates. But here the $\mathcal{ABA}$ schemes of order $(10,6,4)$ performs much better that the other schemes,

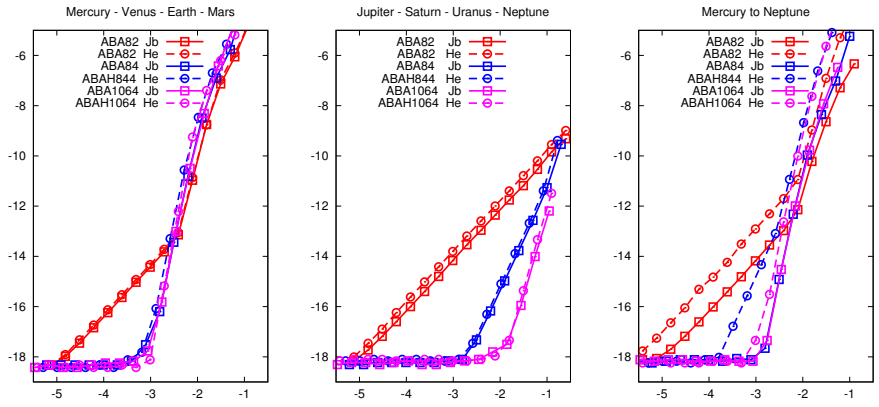

Fig. 7 Comparison between Jacobi (continuous lines) and Heliocentric (discontinous lines) coordinates using the schemes $\mathcal{ABA}82$ (red), $\mathcal{ABA}84$ (blue) and $\mathcal{ABA}1064$ (purple). From left to right: the 4 inner planets, the 4 outer planets and the whole Solar System. The x-axis represents the cost (τ/s) of the method and the y-axis the maximum energy variation for one integration with constant step-size τ.

having an optimal step-sizes one order of magnitude larger than the ones for the schemes of order $(8, 4)$.

If we look at the whole Solar System (Figure 7 right), we see that there is a big difference between taking Jacobi or Heliocentric coordinates. Looking at the $\mathcal{ABA}82$ scheme (red lines) we see that the slopes are the same but that there is a difference of about one order of magnitude in accuracy for a given step-sizes. If we look at the scheme of order $(8, 4)$ (blue lines), we see that in Jacobi coordinates the methods behaves as one of order 8, while in Heliocentric coordinates this one behaves as one of order 4. This can be explained by the difference in the size of the perturbation (see Table 1) in both set of coordinates. We also see that there is a big difference between the optimal step-size for both set of coordinates, making Jacobi coordinates by far the best choice. Finally, if we compare the $\mathcal{ABA}$ schemes of order $(10, 6, 4)$ (purple lines) the difference between the two set of coordinates is drastically reduced, although Jacobi coordinates still perform slightly better. While the extra stages to go from an $(8, 4)$ scheme to a $(10, 6, 4)$ one do not improve in Jacobi coordinates. This is not the case of Heliocentric coordinates, where the $(10, 6, 4)$ gives the best results and the difference between the two set of coordinates is not as relevant as before.

Although Jacobi coordinates presents better results for most of the test models, we believe that using Jacobi or Heliocentric coordinates is a matter of choice.

8 Conclusions

In this article we have reviewed different symplectic splitting schemes and tested their performance for the case of the planetary motion. We recall that in the case of the planetary motion, using an appropriate change of variables, the Hamiltonian of the N - body problem can be rewritten as $H_K + H_I$. A sum of independent

Keplerian motions for each planet (H_K) and a small perturbation term given by the interaction between the planets (H_I).

There are two set of canonical coordinates that allow us to write the Hamiltonian in this way: Jacobi and Heliocentric coordinates (Section 3). Although in Jacobi coordinates the size of the perturbation is smaller and H_I is integrable, Heliocentric coordinates seem more natural and the expressions are easier to handle (Appendix B). In this article we have compared the performance of different symplectic splitting schemes in both set of coordinates.

In Section 5 we described different splitting symplectic schemes for Jacobi coordinates. In Section 6 we saw how to extend these schemes to use Heliocentric coordinates. We note that all the splitting schemes for Jacobi coordinates can also be used in Heliocentric coordinates, but in order to have a comparable performance an extra stage to kill the terms in $\varepsilon^3\tau^2$ must be added (see Section 6).

We have seen that in Jacobi coordinates, the $\mathcal{ABA}84$ scheme introduced by McLachlan (1995) and the $\mathcal{ABA}1064$ scheme Blanes et al (2012) give the best results when we look at the motion of the whole Solar System. The high eccentricity of Mercury and its fast orbital period are the main limiting factors and taking higher order splitting schemes do not always provide significant improvments. But for different planetary configurations, as the 4 outer planets, the $\mathcal{ABA}1064$ has a better performance than the $\mathcal{ABA}84$.

When we consider Heliocentric coordinates, the $\mathcal{ABAH}1064$ (Blanes et al, 2012) gives the best results when we consider the whole Solar System. In this case, probably because the size of the perturbation is larger, adding extra stages to have higher order schemes does improve the results.

Moreover, the performances of the schemes in both set of coordinates, Jacobi or Heliocentric are very similar for the scheme of order $(10, 6, 4)$, with a slight advantage for the Jacobi coordinates. Depending on the problem, one can thus use either system of coordinates, but it is clear that using high order schemes as the $\mathcal{ABA}(\mathcal{H})864$ and $\mathcal{ABA}(\mathcal{H})1064$ Blanes et al (2012) can drastically improve the results. This should be even more the case for highly perturbed systems as some extra solar planetary systems with close planets of large masses.

A On the Compensated Summation

Using any of the symplectic integrating schemes described in this article, we require successive evaluations of $\exp(a_i \tau A)$ and $\exp(b_i \tau B)$. Each of these evaluations slightly modifies the position and velocity of each planet. For τ small, we will have a loss in accuracy due to round-off errors. The *Compensated Summation* is a simple trick that is commonly used to reduce the round-off error. In a general framework, when we consider a numerical method for solving an ODE, we require a recursive evaluation of the form:

$$y_{n+1} = y_n + \delta_n, \tag{26}$$

where y_n is the approximated solution and δ_n is the increment to be done. Usually δ_n will be smaller in magnitude than y_n. In this situation, the rounding errors caused by the computation of δ_n are in general smaller that those to evaluate Eq. 26. The algorithm that can be used in order to reduce this round-off error is called the *"Compensated Summation"* (Kahan, 1965).

Compensated Summation Algorithm: *Let* y_0 *and* $\{\delta_n\}_{n\geq 0}$ *be given and put* $e = 0$. *Compute* $y_1, y_2, \ldots$ *from Eq. 26 as follows:*

$$\begin{array}{l} for\ n = 0, 1, 2, \ldots\ do \\ \quad a = y_n \\ \quad e = e + \delta_n \\ \quad y_{n+1} = a + e \\ \quad e = e + (a - y_{n+1}) \\ enddo \end{array}$$

This algorithm accumulates the rounding errors in e and feeds them back into the summation when possible. At each time-step of the integration, when we evaluate $\exp(a_i \tau A)$ or $\exp(b_i \tau B)$, the increment in position and velocity is done using the compensated summation. In Figure 8 we show the results for the $\mathcal{ABA}$ $(2n, 2)$ schemes for $n = 1, 2, 3, 4$ using double (left) and extended precision (right). In both cases we gain almost one order of magnitude in precision when we take into account the compensated summation.

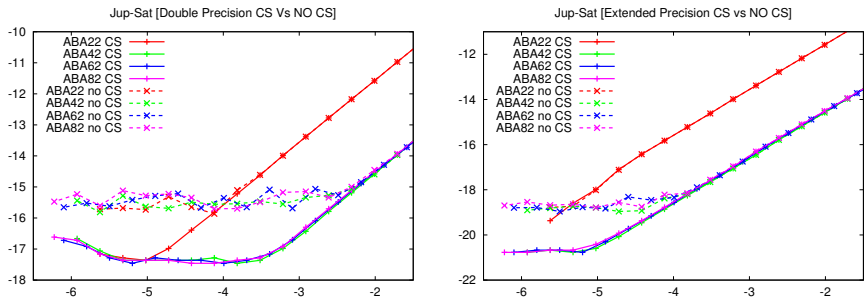

Fig. 8 Comparison between the $\mathcal{ABA}$ schemes of order $(2n, 2)$ for $n = 1, 2, 3, 4$ applied to the Sun-Jupiter-Saturn three body problem. With (CS) and without (noCS) the compensated summation. The x-axis represent the cost (τ/n) and the y-axis the maximum energy variation for one integration with constant step-size τ. Left: using a double precision arithmetics; Right: using an extended precision arithmetics.

B Integration Schemes (*some help on the practical coding*)

In this paper we have reviewed many splitting symplectic integrating schemes, all of them of the form:

$$\mathcal{S}(\tau) = \exp(a_1\tau A)\exp(b_1\tau B)\ \ldots\ \exp(b_1\tau B)\exp(a_1\tau A), \tag{27}$$

where $\exp(\tau A)$ and $\exp(\tau B)$ can be computed explicitly. They correspond to the integrals of the two different parts of the original Hamiltonian. In this section we show how to compute explicitly $\exp(\tau A)$ and $\exp(\tau B)$ for the particular case of the N-body problem in Jacobi and Heliocentric coordinates. We note that from now on: $\tilde{\mathbf{u}}$ stands for the momenta associated to $\mathbf{u}$ and $\mathbf{u}'$ stands for $d\mathbf{u}/dt$.

B.1 Keplerian Motion (H_K)

We recall that in **Jacobi coordinates**,

$$H_K = \sum_{i=1}^{n}\left(\frac{1}{2}\frac{\eta_i}{\eta_{i-1}}\frac{||\tilde{\mathbf{v}}_\mathbf{i}||^2}{m_i} - G\frac{m_i\eta_{i-1}}{||\mathbf{v_i}||}\right), \tag{28}$$

whereas in **Heliocentric coordinates**,

$$H_K = \sum_{i=1}^{n}\left(\frac{1}{2}||\tilde{\mathbf{r}}_\mathbf{i}||^2\left[\frac{m_0+m_i}{m_0m_i}\right] - G\frac{m_0m_i}{||\mathbf{r_i}||}\right). \tag{29}$$

In both cases H_K is a sum of independent Keplerian motions. In Jacobi coordinates each planet follows an elliptical orbit around the centre on mass of the Sun and the planets that are closer to the Sun, the mass parameter of the system is $\mu_J = G\eta_i$. While in Heliocentric coordinates each planet follows an elliptical orbit around the planet-Sun centre of mass, and the mass parameter of the system is $\mu_H = G(m_0+m_i)$.

It is well known that Kepler problem is integrable, but the solution from time $t = t_0$ to $t = t_0 + \tau$ is expressed in a simple form if we consider action-angle variables. To compute $\exp(\tau L_{H_K})$ we need to be able to compute $(\mathbf{r}(\mathbf{t_0}+\tau), \mathbf{v}(\mathbf{t_0}+\tau))$ from $(\mathbf{r}(\mathbf{t_0}), \mathbf{v}(\mathbf{t_0}))$.

An option is to change to elliptical coordinates, advance the mean anomaly and then return to cartesian coordinates. But this can accumulate a lot of numerical errors as well as it is very expensive in terms of computational cost. Instead we use a similar idea as the Gauss f and g functions (Danby, 1992), where we use an expression for the increment in position and velocities for a given step-size τ, without having to perform any change of coordinates. Let us give some details on how to derive these expressions.

In elliptical coordinates the motion of the two body problem is given by $(a, e, i, \Omega, \omega, E)$, where all of the elements remain fixed except for E that varies following Kepler equation $(n(t-t_p) = M = E - e\sin E)$. Using a reference frame where the orbital plane is given by $Z = 0$, the X-axis is the direction of the perihelion and the Y-axis completes an orthogonal reference system on the orbital plane, the position $(X, Y, 0)$ and velocity $(X', Y', 0)$ are given by:

$$\begin{aligned} X &= a(\cos E - e), \qquad Y = a\sqrt{1-e^2}\sin E, \\ X' &= -\frac{na^2}{r}\sin E, \qquad Y' = \frac{na^2}{r}\sqrt{1-e^2}\cos E, \end{aligned} \tag{30}$$

where $r = a(1 - e\cos E)$ and $n = \mu^{1/2}a^{-3/2}$. The position and velocities on a fixed reference frame are given by:

$$\begin{pmatrix} x & x' \\ y & y' \\ z & z' \end{pmatrix} = \mathcal{R}_3(\Omega)\times\mathcal{R}_1(i)\times\mathcal{R}_3(\omega)\times\begin{pmatrix} X & X' \\ Y & Y' \\ 0 & 0 \end{pmatrix}, \tag{31}$$

where

$$\mathcal{R}_1(\theta) = \begin{pmatrix} 1 & 0 & 0 \\ 0 & \cos\theta & \sin\theta \\ 0 & -\sin\theta & \cos\theta \end{pmatrix}, \text{ and } \mathcal{R}_3(\theta) = \begin{pmatrix} \cos\theta & \sin\theta & 0 \\ -\sin\theta & \cos\theta & 0 \\ 0 & 0 & 1 \end{pmatrix}$$

Notice that

$$\mathcal{R}_3(\Omega) \times \mathcal{R}_1(i) \times \mathcal{R}_3(\omega) = \mathcal{R} \times \mathcal{R}_3(\varpi),$$

where $\varpi = \Omega + \omega$ and $\mathcal{R} = \mathcal{R}_3(\Omega) \times \mathcal{R}_1(i) \times \mathcal{R}_3(-\Omega)$. Given that $\mathcal{R}_1(i) = \mathcal{R}_1(i/2)\mathcal{R}_1(i/2)$ we have that:

$$\mathcal{R} = \begin{pmatrix} 1-2\mathbf{p}^2 & 2\mathbf{pq} & 2\mathbf{p}\chi \\ 2\mathbf{pq} & 1-2\mathbf{q}^2 & -2\mathbf{q}\chi \\ -2\mathbf{p}\chi & 2\mathbf{q}\chi & 1-2\mathbf{p}^2-2\mathbf{q}^2 \end{pmatrix}, \tag{32}$$

where $\mathbf{p} = \sin i/2 \sin \Omega, \mathbf{q} = \sin i/2 \sin \Omega$, and $\chi = \sqrt{1-\mathbf{p}^2-\mathbf{q}^2} = \cos i/2$. From Eq. 31 we have,

$$[\ \mathbf{r(t_0)},\ \mathbf{v(t_0)}\ ] = \mathcal{R} \times \mathcal{R}_3(\varpi) \times \begin{bmatrix} X_0 & X_0' \\ Y_0 & Y_0' \\ 0 & 0 \end{bmatrix} \tag{33}$$

$$[\ \mathbf{r(t_0}+\delta\mathbf{t)},\ \mathbf{v(t_0}+\delta\mathbf{t)}\ ] = \mathcal{R} \times \mathcal{R}_3(\varpi) \times \begin{bmatrix} X_1 & X_1' \\ Y_1 & Y_1' \\ 0 & 0 \end{bmatrix}. \tag{34}$$

Hence,

$$[\ \mathbf{r(t_0}+\delta\mathbf{t)},\ \mathbf{v(t_0}+\delta\mathbf{t)}\ ] = [\ \mathbf{r(t_0)}, \mathbf{v(t_0)}\ ] \begin{bmatrix} X_0 & X_0' \\ Y_0 & Y_0' \end{bmatrix}^{-1} \begin{bmatrix} X_1 & X_1' \\ Y_1 & Y_1' \end{bmatrix} \tag{35}$$

$$= [\ \mathbf{r(t_0)}, \mathbf{v(t_0)}\ ] \begin{bmatrix} a_{11} & a_{12} \\ a_{21} & a_{22} \end{bmatrix}. \tag{36}$$

One can check that,

$$\begin{aligned} a_{11} &= 1 + (\cos(E_1 - E_0) - 1)\frac{a}{r_0}, \\ a_{21} &= \frac{a^{3/2}}{\mu^{1/2}} \sin(E_1 - E_0) - e \sin E_1 + e \sin E_0, \\ a_{12} &= -\frac{\sqrt{a}}{r_0 r_1} \sin(E_1 - E_0), \\ a_{22} &= 1 + (\cos(E_1 - E_0) - 1)\frac{a}{r_1}, \end{aligned} \tag{37}$$

where $r_i = a(1 - e\cos E_i)$ for $i = 0, 1$. We use Kepler's equation to compute $\delta E = E_1 - E_0$ from $\delta t = t_1 - t_0$. Taking $M_i = n(t_i - t_p)$ for $i = 0, 1$, we have that δE is the solution of

$$x - e\cos E \sin x - e \sin E \cos x + e \sin E - n\delta t = 0. \tag{38}$$

Calling $C = \cos \delta E$, $S = \sin \delta E$ and $ce = e\cos E_0$, $se = \sin E_0$ we have that $r_1 = a(1 - ce \cdot C + se \cdot S)$. Now we can rewrite Eq. 37 as:

$$\begin{aligned} a_{11} &= 1 + (C - 1)\frac{a}{r_0}, \\ a_{21} &= \delta t + (S - \delta E)\frac{a^{3/2}}{\mu^{1/2}}, \\ a_{12} &= -\frac{S}{r_0\sqrt{a}(1 - ce \cdot C + se \cdot S)}, \\ a_{22} &= 1 + \frac{C - 1}{1 - ce \cdot C + se \cdot S}. \end{aligned} \tag{39}$$

To summarise, given $\mathbf{r} = \mathbf{r(t_0)}, \mathbf{v} = \mathbf{v(t_0)}$ and defining $r_0 = ||\mathbf{r}||$ and $v_0 = ||\mathbf{v}||$. We find

$$a = r_0/(2 - r_0 v_0^2), \qquad ce = e\cos E_0 = r_0 v_0^2 - 1, \qquad se = e \sin E_0 = \langle \mathbf{r}, \mathbf{v} \rangle / \sqrt{\mu a}.$$

Then we take δt and we use Eq. 38 to find δE. Finally we use Eqs. 36 and 39 to find $\mathbf{r(t_0}+\delta\mathbf{t)}, \mathbf{v(t_0}+\delta\mathbf{t)}$.

B.2 Jacobi Coordinates

We recall that in this set of coordinates the perturbation part is given by:

$$H_I = U_1 = G\left[\sum_{i=1}^{n} m_i\left(\frac{\eta_{i-1}}{||\mathbf{v_i}||} - \frac{m_0}{||\mathbf{r_i}||}\right) - \sum_{0<i<j\leq n}\left(\frac{m_i m_j}{||\mathbf{r_i}-\mathbf{r_j}||}\right)\right]. \tag{40}$$

B.2.1 Computing $\exp(L_{H_I})$*:*

U_1 depends only on the position, hence the equations of motion are given by,

$$\frac{d}{dt}\mathbf{v_k} = \frac{\partial U_1}{\partial\ \tilde{\mathbf{v}}_\mathbf{k}}, \qquad \frac{d}{dt}\tilde{\mathbf{v}}_\mathbf{k} = -\frac{\partial U_1}{\partial\ \mathbf{v_k}}.$$

Using $\tilde{\mathbf{v}}_\mathbf{i} = \dfrac{\eta_{i-1}m_i}{\eta_i}\dot{\mathbf{v}}_\mathbf{i}$ we have

$$\mathbf{v_k}(\tau) = \mathbf{v_k}(\tau_0), \qquad \dot{\mathbf{v}}_\mathbf{k}(\tau) = \dot{\mathbf{v}}_\mathbf{k}(\tau_0) - \tau\frac{\eta_i}{\eta_{i-1}m_i}\frac{\partial U_1}{\partial \mathbf{v_k}}.$$

As the expressions for $\partial U_1/\partial\mathbf{v_k}$ can be a little cumbersome, we compute them separately. When we derive H_I with respect to $\mathbf{v_k}$ we must derive 3 main expressions: $1/||\mathbf{v_i}||$, $1/||\mathbf{r_i}||$ and $1/||\mathbf{r_i}-\mathbf{r_j}||$ for $i<j$. We first give the derivatives of these factors with respect to $\mathbf{v_k}$ and then we will deduce $\partial H_I/\partial\mathbf{v_k}$ for $k=1,\ldots,n$.

$$\frac{\partial}{\partial\mathbf{v_k}}\left(\frac{1}{||\mathbf{v_i}||}\right) = -\frac{\mathbf{v_i}}{||\mathbf{v_i}||^3}\cdot\delta_{i,k}\ , \qquad \text{where}\ \ \delta_{i,k} = \begin{cases} 0 & \text{if}\ \ i\neq k,\\ 1 & \text{if}\ \ i=k.\end{cases}$$

$$\frac{\partial}{\partial\mathbf{v_k}}\left(\frac{1}{||\mathbf{r_i}||}\right) = -\frac{\mathbf{r_i}}{||\mathbf{r_i}||^3}\cdot\xi_{i,k}, \qquad \text{where}\ \ \xi_{i,k} = \begin{cases} 0 & \text{if}\ \ i<k,\\ 1 & \text{if}\ \ i=k,\\ \dfrac{m_k}{\eta_k} & \text{if}\ \ i>k.\end{cases}$$

$$\frac{\partial}{\partial\mathbf{v_k}}\left(\frac{1}{||\mathbf{r_i}-\mathbf{r_j}||}\right) = -\frac{\mathbf{r_i}-\mathbf{r_j}}{||\mathbf{r_i}-\mathbf{r_j}||^3}\cdot\psi_{i,j,k}, \ \text{where}\ \ \psi_{i,j,k} = \begin{cases} \dfrac{\eta_{k-1}}{\eta_k} & \text{if} \quad k=i<j,\\ -\dfrac{m_k}{\eta_k} & \text{if} \quad i<k<j,\\ -1 & \text{if} \quad i<j=k,\\ 0 & \text{else}\ \ (k<i<j,\ \ i<j<k).\end{cases}$$

To compute $\partial U_1/\partial\mathbf{v_k}$ for $k=1,\ldots,n$, we consider separately the cases $k=1$ and $k>1$:

$$\frac{\partial U_1}{\partial\mathbf{v_1}} = G\frac{m_0m_1}{\eta_1}\left[\sum_{i=2}^{n} m_i\frac{\mathbf{r_i}}{||\mathbf{r_i}||^3} + \sum_{i=2}^{n} m_i\frac{\mathbf{r_1}-\mathbf{r_i}}{||\mathbf{r_1}-\mathbf{r_i}||^3}\right].$$

$$\begin{aligned}\frac{\partial U_1}{\partial\mathbf{v_k}} = Gm_k\Bigg[&-\eta_{k-1}\frac{\mathbf{v_k}}{||\mathbf{v_k}||^3} + m_0\frac{\mathbf{r_k}}{||\mathbf{r_k}||^3} + \frac{m_0}{\eta_k}\sum_{i=k+1}^{n} m_i\frac{\mathbf{r_i}}{||\mathbf{r_i}||^3}\\ &+ \frac{\eta_{k-1}}{\eta_k}\sum_{j=k+1}^{n} m_j\frac{\mathbf{r_k}-\mathbf{r_j}}{||\mathbf{r_k}-\mathbf{r_j}||^3} - \sum_{i=1}^{k-1} m_i\frac{\mathbf{r_i}-\mathbf{r_k}}{||\mathbf{r_i}-\mathbf{r_k}||^3} - \frac{1}{\eta_k}\sum_{i=1}^{k-1}\sum_{j=k+1}^{n} m_im_j\frac{\mathbf{r_i}-\mathbf{r_j}}{||\mathbf{r_i}-\mathbf{r_j}||^3}\Bigg].\end{aligned}$$

B.2.2 Computing the Corrector: $\exp(L_{\{\{A,B\},B\}})$

In Section 5.2.1 we described a splitting symplectic schemed where a corrector term was added at the beginning and at the end of each step-size. The corrector term is given by,

$$\exp(-\tau^3\varepsilon^2\frac{c}{2}L_C),$$

with $L_C = L_{\{\{A,B\},B\}}$ and c a constant coefficient that depends on the order of the $\mathcal{ABA}$ scheme.

In Jacobi coordinates A is quadratic in p and B only depends on q so $\{\{A,B\},B\}$ only depends on q and $\{\{A,B\},B\}$ is integrable. We recall that $A = H_{Kep} = T_0 + U_0$ and $B = H_{pert} = U_1$. Hence,

$$\{\{T_0+U_0,U_1\},U_1\} = \{\{T_0,U_1\},U_1\}.$$

Given that $T_0 = \sum_{i=1}^{n} \frac{\eta_i}{\eta_{i-1}m_i}\frac{||\tilde{\mathbf{v}}_\mathbf{i}||^2}{2}$, we have,

$$\{T_0,U_1\} = \sum_{i=1}^{n}\frac{\eta_i}{\eta_{i-1}m_i}\tilde{\mathbf{v}}_\mathbf{i}\frac{\partial U_1}{\partial \mathbf{v_i}},$$

$$\{\{T_0,U_1\},U_1\} = \sum_{i=1}^{n}\frac{\eta_i}{\eta_{i-1}m_i}\left(\frac{\partial U_1}{\partial \mathbf{v_i}}\right)^2.$$

Then the equations of motion for L_C are given by:

$$\mathbf{v_k}(\tau) = \mathbf{v_k}(\tau_0),$$
$$\tilde{\mathbf{v}}_\mathbf{k}(\tau) = \tilde{\mathbf{v}}_\mathbf{k}(t_0) + \tau\sum_{i=1}^{n} 2\gamma_i\frac{\partial U_1}{\partial \mathbf{v_i}}\frac{\partial^2 U_1}{\partial \mathbf{v_i}\partial \mathbf{v_k}},$$

where $\gamma_k = \frac{\eta_k}{\eta_{k-1}m_k}$. As before, using $\tilde{\mathbf{v}}_\mathbf{i} = \frac{\eta_{i-1}m_i}{\eta_i}\dot{\mathbf{v}}_\mathbf{i}$ we have

$$\dot{\mathbf{v}}_\mathbf{k}(\tau) = \dot{\mathbf{v}}_\mathbf{k}(t_0) + \tau\gamma_k\sum_{i=1}^{n} 2\left(\gamma_i\frac{\partial U_1}{\partial \mathbf{v_i}}\right)\frac{\partial^2 U_1}{\partial \mathbf{v_i}\partial \mathbf{v_k}}.$$

Again the expression for $\frac{\partial^2 U_1}{\partial \mathbf{v_i}\partial \mathbf{v_k}}$ are a little cumbersome and we first show how to derive the different parts in $\frac{\partial U_1}{\partial \mathbf{v_k}}$: $\mathbf{v_i}/||\mathbf{v_i}||^3$, $\mathbf{r_i}/||\mathbf{r_i}||^3$ and $\mathbf{r_i}-\mathbf{r_j}/||\mathbf{r_i}-\mathbf{r_j}||^3$.

$$\frac{\partial}{\partial \mathbf{v_k}}\left(\frac{\mathbf{v_i}}{||\mathbf{v_i}||^3}\right) = \left(\frac{\langle \mathbf{h},\mathbf{k}\rangle}{||\mathbf{v_i}||^3} - 3\frac{\langle \mathbf{v_i},\mathbf{h}\rangle\langle \mathbf{v_i},\mathbf{k}\rangle}{||\mathbf{v_i}||^5}\right)\cdot\delta_{i,k},$$

$$\frac{\partial}{\partial \mathbf{v_k}}\left(\frac{\mathbf{r_i}}{||\mathbf{r_i}||^3}\right) = \left(\frac{\langle \mathbf{h},\mathbf{k}\rangle}{||\mathbf{r_i}||^3} - 3\frac{\langle \mathbf{r_i},\mathbf{h}\rangle\langle \mathbf{r_i},\mathbf{k}\rangle}{||\mathbf{r_i}||^5}\right)\cdot\xi_{i,k},$$

$$\frac{\partial}{\partial \mathbf{v_k}}\left(\frac{\mathbf{r_i}-\mathbf{r_j}}{||\mathbf{r_i}-\mathbf{r_j}||^3}\right) = \left(\frac{\langle \mathbf{h},\mathbf{k}\rangle}{||\mathbf{r_i}-\mathbf{r_j}||^3} - 3\frac{\langle \mathbf{r_i}-\mathbf{r_j},\mathbf{h}\rangle\langle \mathbf{r_i}-\mathbf{r_j},\mathbf{k}\rangle}{||\mathbf{r_i}-\mathbf{r_j}||^5}\right)\cdot\psi_{i,j,k}.$$

From now on we call $\mathbf{Acc}(i) = \gamma_i\frac{\partial U_1}{\partial \mathbf{v_i}}$, and

$$\Lambda_s = \mathbf{Acc}(s)\left(\frac{\langle \mathbf{h},\mathbf{k}\rangle}{||\mathbf{v_i}||^3} - 3\frac{\langle \mathbf{v_i},\mathbf{h}\rangle\langle \mathbf{v_i},\mathbf{k}\rangle}{||\mathbf{v_i}||^5}\right),$$

$$\Theta_{i,s} = \mathbf{Acc}(s)\left(\frac{\langle \mathbf{h},\mathbf{k}\rangle}{||\mathbf{r_i}||^3} - 3\frac{\langle \mathbf{r_i},\mathbf{h}\rangle\langle \mathbf{r_i},\mathbf{k}\rangle}{||\mathbf{r_i}||^5}\right),$$

$$\Psi_{i,j,s} = \mathbf{Acc}(s)\left(\frac{\langle \mathbf{h},\mathbf{k}\rangle}{||\mathbf{r_i}-\mathbf{r_j}||^3} - 3\frac{\langle \mathbf{r_i}-\mathbf{r_j},\mathbf{h}\rangle\langle \mathbf{r_i}-\mathbf{r_j},\mathbf{k}\rangle}{||\mathbf{r_i}-\mathbf{r_j}||^5}\right).$$

We can now give the expressions for $\dfrac{\partial^2 U_1}{\partial \mathbf{v_i}\partial \mathbf{v_k}}\ \forall j,k$

$$\frac{\partial^2 U_1}{\partial \mathbf{v_1}\partial \mathbf{v_1}} = G\frac{m_0 m_1}{\eta_1}\left[\sum_{j=2}^{n} m_j(\Theta_{j,1}\frac{m_1}{\eta_1} + \Psi_{1,j,1}\frac{m_0}{\eta_1})\right].$$

$$\frac{\partial^2 U_1}{\partial \mathbf{v_1}\partial \mathbf{v_k}} = G\frac{m_0 m_1 m_k}{\eta_1}\left[\Theta_{k,s} - \Psi_{1,k,s} + \frac{1}{\eta_k}\sum_{j=k+1}^{n} m_j(\Theta_{j,s} - \Psi_{1,j,s})\right].$$

$$\begin{aligned}\frac{\partial^2 U_1}{\partial \mathbf{v_k}\partial \mathbf{v_k}} = G m_k\Bigg[&-\eta_{k-1}\Lambda_k + m_0\Theta_{k,k} + \frac{m_0 m_k}{\eta_k^2}\sum_{i=k+1}^{n} m_i\Theta_{i,k} + \frac{\eta_{k-1}^2}{\eta_k^2}\sum_{i=k+1}^{n} m_i\Psi_{k,i,k}\\ &+\sum_{i=1}^{k-1} m_i\Psi_{i,k,k} + \frac{m_k}{\eta_k^2}\sum_{i=1}^{k-1}\sum_{j=i+1}^{n} m_i m_j\Psi_{i,j,k}\Bigg].\end{aligned}$$

$$\begin{aligned}\frac{\partial^2 U_1}{\partial \mathbf{v_k}\partial \mathbf{v_l}} = G\frac{m_k m_l}{\eta_k}\Bigg[&m_0\Theta_{l,s} - \eta_{k-1}\Psi_{k,l,s} + \frac{1}{\eta_l}\sum_{i=l+1}^{n} m_i(m_0\Theta_{i,s} - \eta_{k-1}\Psi_{k,i,s})\\ &+\sum_{i=1}^{k-1} m_i\Psi_{i,l,s} + \frac{1}{\eta_l}\sum_{i=1}^{k-1}\sum_{j=l+1}^{n} m_i m_j\Psi_{i,j,k}\Bigg].\end{aligned}$$

B.3 Heliocentric Coordinates

We recall that in this set of coordinates the perturbation part is given by:

$$H_I = T_1 + U_1 = \sum_{0<i<j\leq n}\frac{\tilde{\mathbf{r}}_\mathbf{i}\cdot\tilde{\mathbf{r}}_\mathbf{j}}{m_0} - G\sum_{0<i<j\leq n}\frac{m_i m_j}{\Delta_{ij}}, \tag{41}$$

B.3.1 Computing $\exp(\tau L_{T_1})$*:*

Notice that T_1 depends only on the momenta $(\tilde{\mathbf{r}})$. Hence, the equations of motion are given by,

$$\frac{d}{dt}\mathbf{r_k} = \frac{\partial T_1}{\partial\,\tilde{\mathbf{r}}_\mathbf{k}} = \sum_{j=1,j\neq k}\frac{\tilde{\mathbf{r}}_\mathbf{j}}{m_0} = \sum_{j=1,j\neq k}\frac{m_j\dot{\mathbf{r}}_\mathbf{j}}{m_0},$$

$$\frac{d}{dt}\tilde{\mathbf{r}}_\mathbf{k} = \frac{\partial T_1}{\partial\,\mathbf{r_k}} = 0.$$

Finally,

$$\mathbf{r_k}(\tau) = \mathbf{r_k}(\tau_0) + \tau\sum_{j=1,j\neq k}\frac{m_j\dot{\mathbf{r}}_\mathbf{j}}{m_0}, \qquad \dot{\mathbf{r}}_\mathbf{k}(\tau) = \dot{\mathbf{r}}_\mathbf{k}(\tau_0).$$

B.3.2 Computing $\exp(\tau L_{U_{pert}})$*:*

Notice that U_1 depends only on the positions $(\mathbf{r})$. Hence, the equations of motion are given by,

$$\frac{d}{dt}\tilde{\mathbf{r}}_\mathbf{k} = \frac{\partial U_1}{\partial\,\mathbf{r_k}} = 0,$$

$$\frac{d}{dt}\tilde{\mathbf{r}}_\mathbf{k} = -\frac{\partial U_1}{\partial\,\mathbf{r_k}} = -G\left(\sum_{j=1}^{k-1}\frac{m_k m_j}{\Delta_{kj}^3}(\mathbf{r_k}-\mathbf{r_j}) - \sum_{j=k+1}^{n}\frac{m_k m_j}{\Delta_{jk}^3}(\mathbf{r_j}-\mathbf{r_k})\right).$$

Given that $\tilde{\mathbf{r}}_\mathbf{k} = m_k \dot{\mathbf{r}}_\mathbf{k}$, we have:

$$\mathbf{r_k}(\tau) = \mathbf{r_k}(\tau_0), \qquad \dot{\mathbf{r}}_\mathbf{k}(\tau) = \dot{\mathbf{r}}_\mathbf{k}(\tau_0) - \tau\ G \left(\sum_{j=1}^{k-1} \frac{m_j}{\Delta_{kj}^3}(\mathbf{r_k} - \mathbf{r_j}) + \sum_{j=k+1}^{n} \frac{m_j}{\Delta_{kj}^3}(\mathbf{r_k} - \mathbf{r_j}) \right).$$

C Heliocentric Coordinates *(Alternatives for the set of equations)*

The canonical Heliocentric coordinates used in Section 6 are canonical and the position of each body is taken with respect to the position of the Sun. The position and their associated momenta are given by:

$$\left.\begin{array}{l} \mathbf{r_0} = \mathbf{u_0} \\ \mathbf{r_i} = \mathbf{u_i} - \mathbf{u_0} \end{array}\right\}, \qquad \left.\begin{array}{l} \tilde{\mathbf{r}}_\mathbf{0} = \tilde{\mathbf{u}}_\mathbf{0} + \cdots + \tilde{\mathbf{u}}_\mathbf{n} \\ \tilde{\mathbf{r}}_\mathbf{i} = \tilde{\mathbf{u}}_\mathbf{i} \end{array}\right\}.$$

The main difference between Jacobi and Heliocentric coordinates is that in the second set of coordinates the kinetic energy is not diagonal in the momenta. Instead we have:

$$T = \frac{1}{2}\sum_{i=0}^{n} \frac{||\tilde{\mathbf{u}}_\mathbf{i}||^2}{m_i} = \frac{1}{2}\sum_{i=1}^{n} \frac{||\tilde{\mathbf{r}}_\mathbf{i}||^2}{m_i} + \frac{1}{2}\frac{||\sum_{i=1}^{n} \tilde{\mathbf{r}}_\mathbf{i}||^2}{m_0}, \tag{42}$$

which can be rewritten as:

$$T = \frac{1}{2}\sum_{i=0}^{n} \frac{||\tilde{\mathbf{u}}_\mathbf{i}||^2}{m_i} = \frac{1}{2}\sum_{i=1}^{n} ||\tilde{\mathbf{r}}_\mathbf{i}||^2 \left[\frac{1}{m_0} + \frac{1}{m_i}\right] + \sum_{0<i<j} \frac{\tilde{\mathbf{r}}_\mathbf{i} \cdot \tilde{\mathbf{r}}_\mathbf{j}}{m_0}. \tag{43}$$

The extra term due to the momenta of the Sun is added to the perturbation part and makes it depend on both position and velocities. In Section 3 we used Eq.43 to derive the Hamiltonian expression. Duncan et al (1998); Chambers (1999); Wisdom (2006) used Eq. 42 instead. Here we discuss the main differences between the two sets of equations and compare the performance of the integrators presented in this paper for both expressions.

C.1 Two different expressions for Heliocentric coordinates

As we know in Heliocentric coordinates the Hamiltonian for an n-planetary system takes the form:

$$H = H_K + T_1 + U_1,$$

a sum of Keplerian parts, a quadratic term in the momenta and the gravitational interaction between the other planets. Using Eq. 43 we have,

$$H_K = \sum_{i=1}^{n} \left(\frac{1}{2}||\tilde{\mathbf{r}}_\mathbf{i}||^2 \left[\frac{m_0 + m_i}{m_0 m_i}\right] - G\frac{m_0 m_i}{||\mathbf{r_i}||} \right), \tag{44}$$

$$T_1 = \sum_{0<i<j\leq n} \frac{\tilde{\mathbf{r}}_\mathbf{i} \cdot \tilde{\mathbf{r}}_\mathbf{j}}{m_0}, \tag{45}$$

$$U_1 = -G \sum_{0<i<j\leq n} \frac{m_i m_j}{\Delta_{ij}}. \tag{46}$$

The main advantage of this way to split the equations is that Kepler's third law is satisfied for the individual planets: $n^2 a^3 = G(m_0 + m_i)$. But $H_I = T_1 + U_1$ is not integrable and $\{T_1, U_1\} \neq 0$.

Using Eq. 42 we have the splitting introduced by Chambers (1999),

$$H_K^* = \sum_{i=1}^{n} \left(\frac{1}{2} \frac{||\tilde{\mathbf{r}}_\mathbf{i}||^2}{m_i} - G \frac{m_0 m_i}{||\mathbf{r_i}||} \right), \tag{47}$$

$$T_1^* = \frac{1}{2} \frac{||\sum_{i=1}^{n} \tilde{\mathbf{r}}_\mathbf{i}||^2}{m_0}, \tag{48}$$

$$U_1^* = -G \sum_{0<i<j\leq n} \frac{m_i m_j}{\Delta_{ij}}. \tag{49}$$

With this way to split the equations the mass parameter for the Keplerian orbits is $\mu = Gm_0$ for all of the planets. On the other hand, T_1^* and U_1^* (Eqs. 48-49) commute, i.e. $\{T_1^*, U_1^*\} = 0$ and this is a advantage when we build high order splitting schemes. For simplicity let us consider $H_B = T_1$ and $H_C = U_1$ for both expressions. We recall that in Heliocentric coordinates we need to integrate $\exp(\tau(B + C))$. Using Chambers' splitting (Eqs. 48-49) we have:

$$\exp(\tau(B + C)) = \exp(\tau B) \exp(\tau C), \tag{50}$$

which can be computed exactly and does not introduce any extra error terms to the splitting schemes discussed in Section 5. Instead using the first splitting expressions (Eqs. 45-46) we used

$$\exp(\tau(B + C)) \approx \exp(\frac{\tau}{2} C) \exp(\tau B) \exp(\frac{\tau}{2} C), \tag{51}$$

and introduced error terms of order $\varepsilon^3\tau^2$. To deal with this in Section 6 derived splitting schemes where an extra stage was added to get rid of these extra error terms.

C.2 Comparisons between the expressions

We recall that when we use Chambers expression (Eqs. 47-49) we use the splitting schemes discussed in Section 5 with

$$\mathcal{S}(\tau) = \prod_{i=1}^{n} \exp(a_i \tau L_{H_{K^*}}) \exp(b_i \tau L_{T_1^*}) \exp(b_i \tau L_{U_1^*}). \tag{52}$$

While when we use the classical expression (Eqs. 44-46) we use the splitting schemes discussed in Section 6 with

$$\mathcal{S}(\tau) = \prod_{i=1}^{n} \exp(a_i \tau L_{H_{Kep}}) \exp(b_i \frac{\tau}{2} L_{T_1}) \exp(b_i \tau L_{U_1}) \exp(b_i \frac{\tau}{2} L_{T_1}). \tag{53}$$

We compare the $\mathcal{ABA}$ schemes of orders $(8, 2)$, $(8, 4)$ and $(10, 6, 4)$ for both splitting expressions. We recall that the schemes of order $(8, 4)$ and $(10, 6, 4)$ that use the classical splitting (Eqs. 44-46) have one more stage than the schemes used with Chambers splitting (Eqs. 47-49).

Figure 9 summarise the performance of the different integrating schemes presented in Sections 5 and 6. From left to right we have the results for the inner planets, the outer planets and the whole Solar System. The red lines show the performance of the $\mathcal{ABA}82$ scheme, the green lines are for the $\mathcal{ABA}84$ schemes and the blue lines are for the $\mathcal{ABA}1064$ schemes. We use continuous lines when we consider the classical splitting and discontinuous lines for Chambers splitting.

As we can see, there is no significant difference between using one splitting or the other. In some cases one is better that the other. The main advantage that the splitting introduced by Chambers is that we do not require and extra stage for a high-order scheme.

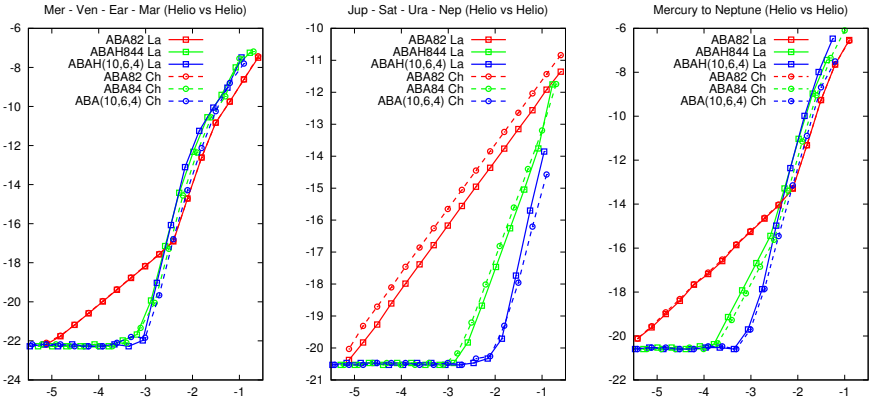

Fig. 9 Comparison between the two expressions for Heliocentric coordinates: the classical expression (Eqs. 44-46) continuous lines and the Chambers expression (Eq. 47-49) discontinuous lines. For the schemes $\mathcal{ABA}82$ (red), $\mathcal{ABA}84$ (green) and $\mathcal{ABA}1064$ (blue). From left to right: the 4 inner planets, the 4 outer planets and the whole Solar System. The x-axis represents the cost (τ/s) of the method and the y-axis the maximum energy variation for one integration with constant step-size τ.

D Comparison in Quadruple Precision

As we have discussed throughout the article, in many cases we have seen that despite taking higher order methods no significant improvement on the performance of the schemes was observed. This is the case of the 4 inner planets in the Solar System, where the size of the perturbation is so small that the extra stages to increase the order of the schemes are useless. Here the round-off error dominates the terms in ε^2 and ε^4. Similar results are also observed when we consider the whole Solar System. In order to see an improvement we need to use higher precision arithmetics. Here we have repeated the test from Sections 5 and 6 for the different integrating schemes using quadruple precision arithmetics. We want to illustrate that the different schemes of orders $(8,6,4)$ and $(10,6,4)$ perform better that those of order $(8,4)$.

In Figures 10 and 11 we show the results for the same test models used throughout the article for Jacobi and Heliocentric coordinates respectively using quadruple precision arithmetics. For Jacobi coordinates (Figure 10) we compare the $\mathcal{ABA}82$, $\mathcal{ABA}84$, $\mathcal{ABA}104$, $\mathcal{ABA}864$ and $\mathcal{ABA}1064$ schemes. For Heliocentric coordinates (Figure 11) we compare the $\mathcal{ABAH}82$, $\mathcal{ABAH}84$, $\mathcal{ABAH}864$ and $\mathcal{ABAH}1064$. As we can see in Figure 10 for Jacobi coordinates, the $\mathcal{ABA}864$ and $\mathcal{ABA}1064$ (Blanes et al, 2012) do improve the performance of the $\mathcal{ABA}84$ (McLachlan, 1995). Notice also that for the 4 inner planets (Figure 10 left) and the whole Solar System (Figure 10 right) the improvement is achieved for small step-sizes, where the energy variation is bellow the machines epsilon for extended arithmetics precision. In Figure 11 similar results are observed for Heliocentric coordinates.

From these experiments we see how the $\mathcal{ABA}$ splitting methods of orders $(8,6,4)$ and $(10,6,4)$ for both set of coordinates improve the performance of the McLachlan (1995) $\mathcal{ABA}84$ and the Laskar and Robutel (2001) $\mathcal{ABA}82$.

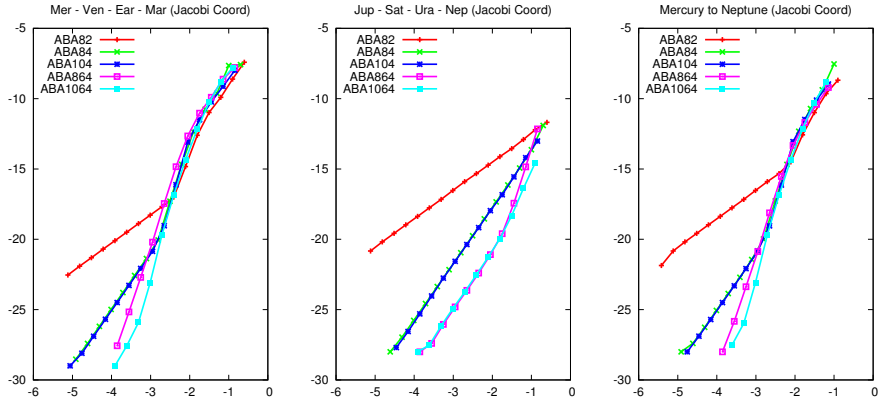

Fig. 10 Comparison using Jacobi coordinates between the $\mathcal{ABA}82$, $\mathcal{ABA}84$, $\mathcal{ABA}104$, $\mathcal{ABA}864$ and $\mathcal{ABA}1064$ schemes using quadruple precision arithmetics. From left to right: the 4 inner planets, the 4 outer planets and the whole Solar System. The x-axis represents the cost (τ/s) and the y-axis the maximum energy variation for one integration with constant step-size τ.

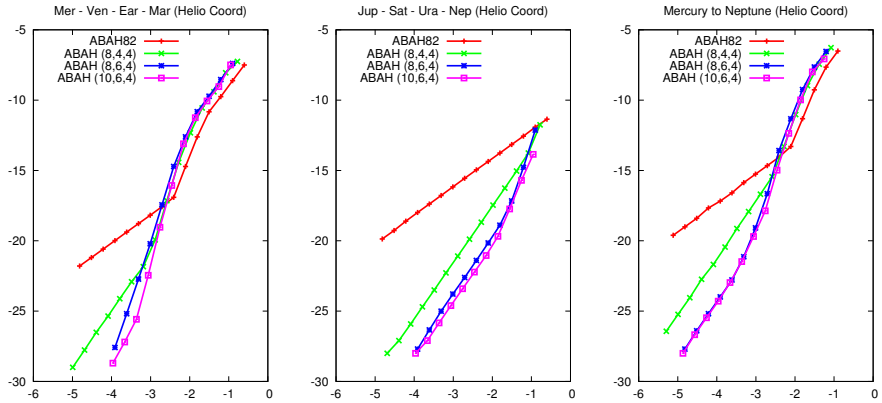

Fig. 11 Comparison using Heliocentric coordinates between the $\mathcal{ABAH}82$, $\mathcal{ABAH}84$, $\mathcal{ABAH}864$ and $\mathcal{ABAH}1064$ schemes using quadruple precision arithmetics. From left to right: the 4 inner planets, the 4 outer planets and the whole Solar System. The x-axis represents the cost (τ/s) and the y-axis the maximum energy variation for one integration with constant step-size τ.

Acknowledgements This work was supported by GTSNext project. The work of SB, FC, JM and AM has been partially supported by Ministerio de Ciencia e Innovación (Spain) under project MTM2010-18246-C03 (co-financed by FEDER Funds of the European Union).

References

Blanes S, Casas F, Farrés A, Laskar J, Makazaga J, Murua A (2012) New families of symplectic splitting methods for numerical integration in dynamical astronomy. Submitted

Chambers JE (1999) A hybrid symplectic integrator that permits close encounters between massive bodies. Monthly Notices of the Royal Astronomical Society 304:793–799, DOI 10.1046/j.1365-8711.1999.02379.x

Chambers JE, Murison MA (2000) Pseudo-high-order symplectic integrators. The Astronomical Journal 119(1):425

Danby JMA (1992) Fundamentals of Celestial Mechanics, Willmann-Bell, p 483

Duncan MJ, Levison HF, Lee MH (1998) A Multiple Time Step Symplectic Algorithm for Integrating Close Encounters. Astronomical Journal 116:2067–2077, DOI 10.1086/300541

Goldman D, Kaper T (1996) Nth-order operator splitting schemes and nonreversible systems. SIAM J Numer Anal 33:349–367

Hairer E, Lubich C, Wanner G (2006) Geometric Numerical Integration. Structure-Preserving Algorithms for Ordinary Differential Equations, Second edn. Springer-Verlag

Kahan W (1965) Pracniques: further remarks on reducing truncation errors. Commun ACM 8:40–, DOI 10.1145/363707.363723

Kinoshita H, Yoshida H, Nakai H (1991) Symplectic integrators and their application to dynamical astronomy. Celestial Mechanics and Dynamical Astronomy 50:59–71

Koseleff PV (1993) Relations among lie formal series and construction of symplectic integrators. In: Cohen G MT, O M (eds) in Applied Algebra, Algebraic Algorithms and Error Correcting Codes (AAECC-10), Springer Verlag, New York, Lect. Not. Comp. Sci, vol 673, pp 213–230

Koseleff PV (1996) Exhaustive search of symplectic integrators using computer algebra. Fields Institute Communications 10

Laskar J (1989) A numerical experiment on the chaotic behaviour of the solar system. Nature 338:237, URL `http://adsabs.harvard.edu/abs/1989Natur.338..237L`

Laskar J (1990a) The chaotic motion of the solar system - a numerical estimate of the size of the chaotic zones. Icarus 88:266–291, URL `http://adsabs.harvard.edu/abs/1990Icar...88..266L`

Laskar J (1990b) Les Méthodes Modernes de la Mecánique Céleste (Goutelas, France, 1989), Editions Frontières, chap Systèmes de Variables et Eléments, pp 63–87

Laskar J, Robutel P (2001) High order symplectic integrators for perturbed hamiltonian systems. Celestial Mechanics and Dynamical Astronomy 80:39–62, 10.1023/A:1012098603882

Laskar J, Quinn T, Tremaine S (1992) Confirmation of resonant structure in the solar system. Icarus 95:148–152, DOI DOI:10.1016/0019-1035(92)90196-E, URL http://adsabs.harvard.edu/abs/1992Icar...95..148L

Laskar J, Robutel P, Joutel F, Gastineau M, Correia ACM, Levrard B (2004) A long-term numerical solution for the insolation quantities of the earth. Astronomy and Astrophysics 428:261–285

Laskar J, Fienga A, Gastineau M, Manche H (2011a) La2010: a new orbital solution for the long-term motion of the earth. Astronomy and Astrophysics 532:89, DOI DOI:10.1051/0004-6361/201116836;eprintid:arXiv:1103.1084

Laskar J, Gastineau M, Delisle JB, Farrés A, Fienga A (2011b) Strong chaos induced by close encounters with ceres and vesta. Astronomy and Astrophysics 532:L4, DOI DOI:10.1051/0004-6361/201117504

Lourens L, Hilgen F, Laskar J, Shackleton N, Wilson D (2004) The neogene period. In: Gradstein F, Ogg J, Smith A (eds) A Geological Timescale 2004, pp 409–440

McLachlan R, Quispel R (2002) Splitting methods. Acta Numerica 11:341–434

McLachlan RI (1995) Composition methods in the presence of small parameters. BIT Numerical Mathematics 35:258–268, 10.1007/BF01737165

McLachlan RI (2002) Families of high-order composition methods. Numerical Algorithms 31:233–246

Milankovitch M (1941) Kanon der Erdbestrahlung und seine Anwendung auf das Eiszeitenproblem. Spec. Acad. R. Serbe, Belgrade

Morbidelli A (2002) Modern integrations of solar system dynamics. Annual Review of Earth and Planetary Sciences 30:89–112, DOI DOI:10.1146/annurev.earth.30.091201.140243, URL http://adsabs.harvard.edu/abs/2002AREPS..30...89M

Murua A, Sanz-Serna J (1999) Order conditions for numerical integrators obtained by composing simpler integrators. Philosophical Transactions of the Royal Society of London Series A: Mathematical, Physical and Engineering Sciences 357(1754):1079–1100, DOI 10.1098/rsta.1999.0365, URL http://rsta.royalsocietypublishing.org/content/357/1754/1079.abstract, http://rsta.royalsocietypublishing.org/content/357/1754/1079.full.pdf+html

Quinn TR, Tremaine S, Duncan M (1991) A three million year integration of the earth's orbit. The Astronomical Journal 101:2287–2305, URL http://adsabs.harvard.edu/abs/1991AJ....101.2287Q

Saha P, Tremaine S (1994) Long-term planetary integration with individual time steps. Astronomical Journal 108:1962–1969, DOI 10.1086/117210, arXiv:astro-ph/9403057

Sheng Q (1989) Solving linear partial differential equations by exponential splitting. IMA J Numer Anal 9:199–212

Sussman GJ, Wisdom J (1992) Chaotic evolution of the solar system. Science 257:56–62, URL http://adsabs.harvard.edu/abs/1992Sci...257...56S

Suzuki M (1990) Fractal decomposition of exponential operators with applications to many-body theories and monte carlo simulations. Physics Letters A 146(6):319 – 323, DOI 10.1016/0375-9601(90)90962-N

Suzuki M (1991) General theory of fractal path integrals with applications to many-body theories and statistical physics. Journal of Mathematical Physics 32(2):400–407

Viswanath D (2002) How Many Timesteps for a Cycle? Analysis of the Wisdom-Holman Algorithm. BIT Numerical Mathematics 42:194–205

Wisdom J (2006) Symplectic correctors for canonical heliocentric n-body maps. The Astronomical Journal 131(4):2294

Wisdom J, Holman M (1991) Symplectic maps for the n-body problem. Astronomical Journal 102:1528–1538, DOI 10.1086/115978

Wisdom J, Holman M, Touma J (1996) Symplectic Correctors. Fields Institute Communications, Vol 10, p 217 10:217–+

Yoshida H (1990) Construction of higher order symplectic integrators. Physics Letters A 150(5-7):262 – 268, DOI 10.1016/0375-9601(90)90092-3